KTH Industrial Engineering and Management

Safe, Sustainable Discharge of Electric Vehicle Batteries as a Pre-treatment Step to Crushing in the Recycling Process

Nicole Shantelle Nembhard

Master of Science Thesis

KTH School of Industrial Engineering and Management
Energy Technology ITM-EX 2019:390
Division of Heat and Power Technology
SE-100 44 STOCKHOLM

Master of Science Thesis ITM-EX 2019:390

KTH Industrial Engineering and Management

Safe, Sustainable Discharge of Electric Vehicle Batteries as a Pre-treatment Step to Crushing in the Recycling Process

Nicole Nembhard

Approved	Examiner Justin Chiu	Supervisor Justin Chiu
	Commissioner Northvolt AB	Contact person Ingrid Karlsson

Abstract

According to the Intergovernmental Panel on Climate Change, an increase in global temperature to above 1.5°C can be halted but would require immediate intervention to reach net zero emissions in the next 15 years. This intervention would have to make use of sustainable energy technologies such as net-zero carbon systems for automobiles. Electric vehicle (EV) use is set to increase 3000% between 2016 and 2030. Due to the inherent toxicity of the chemicals within Li-ion batteries, they must be recycled to be sustainable. Recycling using energy recovering, hydrometallurgical process reduces greenhouse gas emissions. However, due to the high energy and power density within EV batteries, discharging the batteries is an important safety step in the pre-treatment process.

There is no industry standard for discharging EV batteries. Many processes are suggested in literature with little information as to the methods used. The aim of this thesis is to explore four processes that could be suitable for industrial use. A suitable process should be 'safe', meaning it reduces the risk to the facility by minimizing the fire or explosion hazard, minimizes or eliminates human interaction with the battery pack and limits voltage rebound of an individual cell to 0.5V. The process should also be 'rapid', meaning it ensures that discharging does not become a bottleneck in recycling, 'sustainable' meaning it has no polluting fluid waste streams and 'feasible' that is, is cost efficient.

Three processes were found effective. The first, is a combination of salt-solution and metal powder discharge methods using sodium carbonate and steel. This method is intended for battery packs and modules of less than 500V at 0% SOC. The second, is energy recovering electronic load discharge for battery backs greater than 500V or at greater than 0% SOC. Finally, inductive, wireless discharge with BMS 'override' is suggested. This method is suitable for future battery packs of all sizes equipped with wireless charging technology.

Table of Contents

List of Figures

Nomenclature

A	-Amperes
AC	-Alternating Current
Ah	-Ampere hours
BMS	-Battery Management System
BMU	-Battery Management Unit
CC	-Constant Current
CP	-Constant Power
CR	-Constant Resistance
CV	-Constant Voltage
D	-Length of positive terminal
DC	-Direct Current
EOL	-End of Life
Eq	-equivalent
EV	- Electric Vehicle
$FeSO_4$	-Iron sulphate
GWP	-Global Warming Potential
HEV	- Hybrid Electric Vehicle
I	-Current
IPCC	-Intergovernmental Panel on Climate Change
K_2CO_3	-Potassium Carbonate
kg	-kilogram
kWh	-kilowatt hour
L	-length
LCA	-Life Cycle Analysis
LCO	-Lithium Cobalt Oxide
LFP	-Lithium Iron Phosphate
LIB	-Lithium Ion Battery
Li-ion	-Lithium-ion
m	-meters
Na_2CO_3	-Sodium Carbonate
$NaHCO_3$	-Sodium Hydrogen Carbonate/Sodium Bicarbonate
$NaNO_2$	-Sodium Nitrite
$NaNO_3$	-Sodium Nitrate
Na_2SO_4	-Sodium Sulphate

NCA	-Nickel Cobalt Aluminium
NMC	-Nickel Manganese Cobalt
Q	- Capacity
SOC	-State of Charge
SOH	-State of Health
t	-tonne
V	-Volt
V2G	-Vehicle to Grid
wt	-weight
Z	-Ionic Charge
M	-Ionic Strength
K	-Conductivity
[]	-Concentration

Acknowledgments

I would like to thank:

- My family, particularly my parents for their unrelenting support and advice throughout this process.
- The Northvolt Environmental team for welcoming me to Sweden and for making me feel at home.
- The InnoEnergy SELECT programme for offering me this opportunity and
- All the people I interviewed for this thesis, far too many to name, I hope I have represented you well.

1 Introduction

On October 8, 2018, the Intergovernmental Panel on Climate Change (IPCC) released an alarming report: 'rapid, far-reaching and unprecedented changes in all aspects of society' must be made to limit global warming to 1.5°C. Without doing so, the world will face dire and irreversible consequences: extreme weather, rising sea levels diminishing Arctic Ocean sea ice, complete coral reef decline and loss of land ecosystems (IPCC, 2018).

According to the IPCC, limiting global temperature rise would require immediate intervention to reach net zero emissions in the next 15 years (IPCC, 2018). This intervention would have to make use of sustainable energy technologies to produce energy efficient, net-zero carbon systems for automobiles, electric power generators, and building heating and cooling systems using renewable energy power sources and waste heat recovery (IPCC, 2014).

Net-zero carbon systems for automobiles require a net-zero carbon power source. Electric vehicles (EVs) powered by renewable energy have been tapped as the primary means by which to decarbonize the transport sector. As a result of the push from policymakers and global awareness, the number of electric vehicles bought and used worldwide will increase from 750'000 to 24.4 million, an increase of over 3000% between 2016 and 2030. Due to this upsurge in EV use, in Europe alone, 1.16 million batteries will be at their end of life by 2030 (Drabik & Rizos, 2018). Improperly disposed EV batteries are a threat to the environment, ecosystems and human health, they release toxic heavy metals and harmful gases with global warming potential (Zheng , et al., 2018). Therefore, although EVs decarbonize the transport sector, if their batteries are improperly disposed, they threaten the very eco-system they are meant to protect. So, recycling EV batteries is imperative to meeting the IPCC goals.

Furthermore, several of the elements in the batteries: Lithium, Cobalt, Nickel, Aluminum, Copper and Manganese, are valuable. Cobalt is the most valuable of list at 34'500 €/t (April 23, 2019) (LME, 2019). The price of cobalt is volatile, having increased from 29'000 €/t to the present value in the April alone. This volatility is due to the increasing demand for electric vehicles coupled with socio-political volatility in the largest worldwide supplier, the Democratic Republic of Congo (Drabik & Rizos, 2018). The cathode active material, containing cobalt and the other key metals listed above, makes up around 20% of the cost of an EV battery (Gaines, 2018). It is clear then, that there is also a financial driver for recycling Li-ion batteries.

Current recycling processes follow a sequence of discharging and/or disassembly, hydro or pyrometallurgy, metal extraction and product preparation (Zheng , et al., 2018). Pyrometallurgy or smelting is energy intensive. High temperatures must be achieved to melt the metals, the process does not recover Lithium, Nickel nor Manganese and it emits harmful waste gases. Hydrometallurgy is preceded by crushing followed by several chemical based metal extraction techniques. These chemical techniques can recover not only Lithium but also the organic compounds included in the battery composition (Zheng , et al., 2018) (Wuschke, Jackel, Leissner, & Peuker, 2019). Hydrometallurgy is considered more environmentally friendly than pyrometallurgy, particularly if the chemical waste is well managed. However, for safety reasons, a deep discharge of the batteries is crucial. The anode and cathode materials could meet during the crushing process, thereby causing a short circuit or self-ignition (Li, Wang, & Xu, 2016). At small scales, self-ignition of the cells may not prove dangerous, however, to manage the volume of batteries expected in 2030, deep discharge becomes necessary to avoid explosions and damage to the recycling facility.

Some companies avoid the discharging process by manually dismantling the batteries using personnel trained in high voltage systems and crushing the batteries under cryogenic conditions; processes which pose safety issues, are energy intensive and costly (Sonoc, Jeswiet, & Soo, 2015) . In order to lower the cost and risk of recycling, alternative methods to discharging must be made available. The proposed process must be safe so that there is no human interaction with the battery, must have a short enough duration to not become a bottleneck when a large quantity of batteries enter the facility, must be robust enough to ensure that the risk of self-ignition during crushing is minimized and must be sustainable, lowering global warming potential and other environmental hazards. The aim of this thesis is to evaluate four potential process.

2 Background

2.1 Lithium Ion Batteries

Batteries consist of an anode, cathode, separator and electrolyte, the complete system is referred to as a cell. The anode of a Lithium ion battery (LIB) is typically a graphite film on copper, whilst the cathode is a lithium oxide material on aluminum (Chagnes, 2015). For EVs, the lithium oxide typically consists of either a nickel-cobalt-aluminum oxide (NCA) or a nickel-manganese-cobalt oxide (NMC) (Elwert, et al., 2015). Both the copper and aluminum films act as current collectors. The composition of the electrolyte varies but is often $LiPF_6$ dissolved in an organic solvent.

The electrolyte acts as a conductor allowing the Lithium ions to move between the cathode and the anode and in the reverse, in an oxidation and reduction reaction respectively. The Lithium ions transferring to and from the electrolyte allow for the movement of electrons since the lithium changes state. This movement of electrons converts chemical energy to electrical energy and is a mostly reversible process. The process is provoked by the movement of electrons, that is, by connecting the battery to a load which charges (electrons transfer from anode to cathode) or discharges (electrons transfer from cathode to anode) the battery.

The separator is typically an organic membrane meant to allow the transfer of Lithium ions but not allow a short circuit between the anode and cathode. The difference between the stored electrons on the cathode side and the electron holes on the anode side is what is measured as the electrostatic potential or the voltage of the battery. The typical Lithium ion battery cell operates between 2.5V and 4V. Within this region, the process of charging and discharging is reversible. Outside of this region, other processes take place that destroy the cathode material or copper film making it unable to supply or receive Lithium ions when charging or discharging (Chagnes, 2015).

A cylindrical Lithium-ion battery cell (see Figure 1) consists of the jelly roll, the casing, current collectors or terminals and various safety devices. The jelly roll is the progression of anode, separator and cathode rolled up like the Swiss Jelly Roll pastry. The positive terminal is connected to the cathode by an aluminum tab whereas the negative terminal is connected by a copper tab to the anode. The tab of the negative terminal is connected to the casing, so almost the entire casing is the negative terminal except the cap, which is the positive terminal; separated from the negative by a polymer gasket. The casing is typically nickel-plated steel, a highly corrosion resistant material. The positive terminal is easily identified as the non-flat side of the cell. The other components of the cell are exhaust gas holes for venting during thermal runaway and insulation plates between the jelly roll and the casing, to avoid a short circuiting (The Pennsylvania State University, 2014).

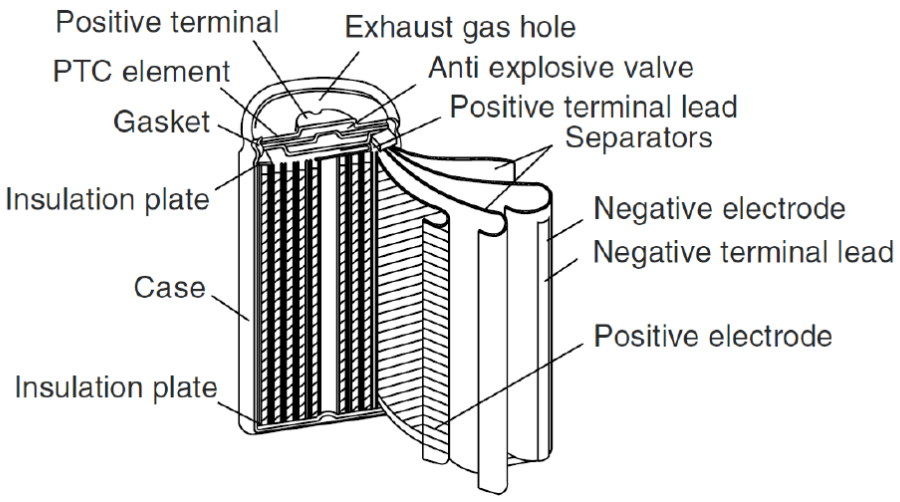

Figure 1: Cylindrical Lithium Ion cell (The Pennsylvania State University, 2014)

Batteries are characterized by their capacity and operating voltage. The operating voltage of a cell is limited by the potential difference across the terminals of the battery when no current is being drawn, also known as the open circuit voltage (Voc). The magnitude of the open-circuit voltage is constrained to 5 V because of the difference between the electrochemical potentials of the anode and the cathode and the energies of the electrons. For safe operation, the cell is typically limited to 4.2V. Over a given voltage, a cell can only deliver a specific amount of electric charge or current, this is known as the capacity (Q) of the battery which is measured in ampere hours (Ah). The capacity is limited by the electrode, particularly cathode materials. Naturally, the current or electric charge that can be delivered lessens with decreasing battery voltage. However, a particular benefit of LIBs is that the voltage is linear over a range of capacities. This is known as the nominal voltage of the battery and is the ideal operating range (see Figure 2) (Julien, Mauger, Vijh, & Zaghib, 2016).

The process of discharging a battery is typically discussed in terms of Coulombic rate, where a current equal to the capacity of the battery is known as 1C and the cell would be discharged in one hour. Therefore, a discharge current equal to half the capacity would require two hours to discharge the cell, equivalent to 0.5C and so on. A cell is considered discharged at the end of its operating range, which is typically at 2.5V. Increasing the discharge current affects the performance of the cell by artificially increasing or decreasing the operating range, sometimes making the cell operate to only 80% of its full capacity. Whether a cell is fully charged or not is monitored using the State of Charge (SOC). The SOC is defined as the available electric charge over the full capacity of the battery (Julien, Mauger, Vijh, & Zaghib, 2016).

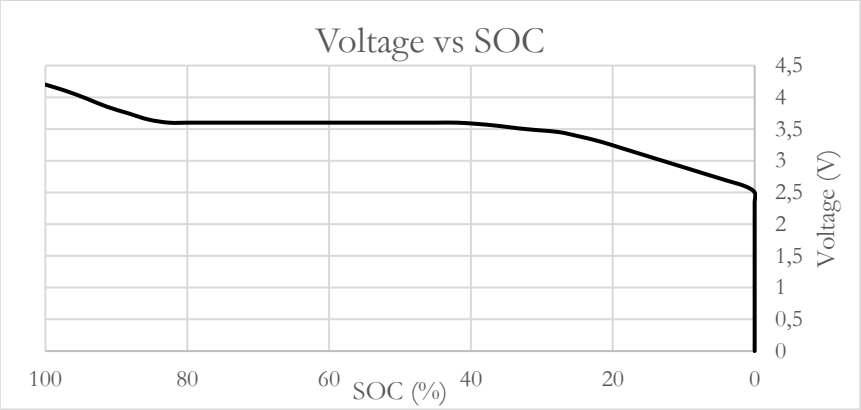

Figure 2: showing open voltage versus state of charge for discharging a battery. The nominal voltage is the nominally horizontal part of the graph.

Self-discharge is the process by which a cell loses electric charge when stored and unused over time due to internal chemical reactions. This issue is more prevalent at full capacity and is asymptotic, meaning there is less self-discharge as the battery loses capacity. Nevertheless, the process is slow at 1-2% of the capacity each month (Battery University, n.d.).

2.2 Electric and Hybrid Electric Vehicles

Although EVs are the focus of this study, other types of batteries can be recycled including batteries for portable electronics, electrification of industrial processes, grid stabilization, home systems and renewables. All these types of batteries can be recycled and should be explored in further work (Battery University, n.d.).

One cell of 4V is not enough to power a vehicle. Typically, cells are connected in series and parallel to increase the voltage and current respectively. This grouping of cells is called a module. A module is usually fitted with a temperature sensor, a current/voltage sensor and a cooling system, all together part of the thermal management system that keeps the module within a safe operating range. The modules are then connected in series to form a battery pack which can be anywhere between 200V for a hybrid electric vehicle to 800V for a full electric vehicle.

The modules are monitored by the battery management system or unit (BMS/BMU). The BMS is an electronic control system connected to the current/voltage and temperature sensors and the thermal management system to monitor the state of health (SOH), balance the state of charge and is connected to fuses and switches in order to protect the battery from over-voltages or over charge/discharge (Kwade & Diekmann, 2018). As batteries become older their capacities decrease and the wire connections to the cells become weak, resulting in a sub-optimal battery operation meaning a poor SOH. The BMS also monitors this behavior for the user and will alert the user when the battery is at a critically poor SOH or is at its end of life (EOL). The battery/car manufacturer would also have access to the readout of the BMS in order to monitor for issues and use the data for future programming (Battery University, n.d.).

Almost 60% of the value of a battery pack is the materials. 30% of the cost of the materials is due solely to the cathode active materials (Gaines, 2018). The battery pack consists of modules, the BMS, cabling, fuses, a circuit board, cooling tubes, current collectors and casing (see Figure 3). The majority of the pack is made of aluminum, steel and plastics, where aluminum is around 30% of the weight of the pack (Diekmann, Hanisch, Loellhoeffel, Schalicke, & Kwade, 2016). All the materials within a battery pack are recyclable with varying degrees of market value from high value materials like the aluminum and copper to less valuable plastics (Elwert, et al., 2015).

Figure 3: showing components of the battery pack. On lower level, from left: aluminum casing, circuit board, aluminum nails, nuts and bolts, copper current collectors, cabling, plastics and modules (Elwert, et al., 2015)

2.3 Safety

The level of risk involved in an LIB battery pack depends on the cathode active material chemistry, the capacity of the cell, the electrical configuration of the pack and the voltage (Brandt & Garche, 2019). A battery is considered high voltage when it exceeds 60V. Battery packs are 200-800V depending on whether they are for a hybrid or full electric vehicle. At high voltage, a battery poses several risks (see Figure 4). One such risk is electrical, since a human in contact with a high voltage circuit can become severely or fatally injured (Brandt & Garche, 2019).

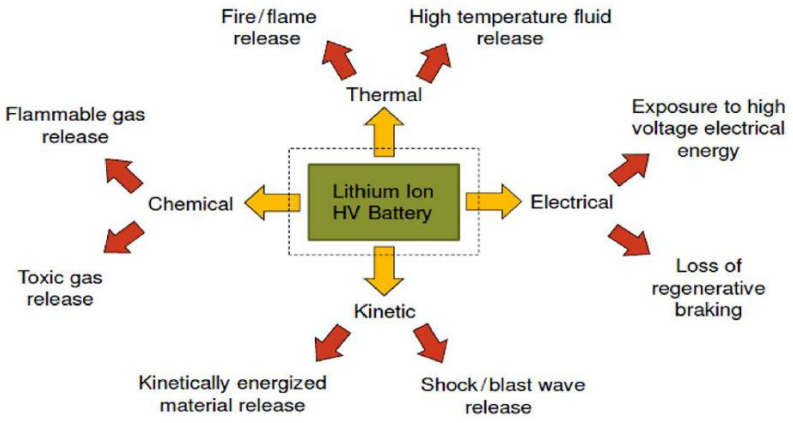

Figure 4: showing Lithium Ion high voltage (HV) battery safety risks grouped into thermal, chemical, kinetic and electrical risks (Brandt & Garche, 2019)

The risk most typically associated with LIBs is thermal and kinetic. Due to their high energy and power density, when triggered by physical abuse, overcharge, internal/external short circuits or high temperatures, there is rapid, uncontrolled release of the stored electrical energy, prompting exothermic chemical reactions caused by the free lithium ions. This process is known as thermal runaway and is most hazardous in batteries near their full capacity (SOC 100%). In thermal runaway, temperatures can arrive at over 800°C causing the cell to open explosively or cause a fire. Cells undergoing thermal runaway often trigger adjacent cells, forcing a chain reaction. Thermal runaway is activated at around 90-200°C (Brandt & Garche, 2019) (Perea, et al., 2018) (Larsson, 2014).

In terms of chemical risk, the electrolyte in NMC and NCA batteries is typically Lithium hexafluorophosphate ($LiPF_6$) dissolved in organic solvents. This electrolyte is corrosive and toxic and reacts violently with water or moisture to produce hydrogen fluoride, phosphorous oxides and lithium oxide (LTS Research Laboratories Inc, 2015). The solvents are also flammable, releasing hydrogen, methane, carbon dioxide and carbon monoxide when heated (Kwade & Diekmann, 2018). Cells are typically equipped with a safety feature called venting. During venting the air around the cells is displaced, which creates an oxygen starved atmosphere where the gases may not ignite, however, if the venting is not quick enough or not activated, gas formation in the cell can cause an increase in the internal pressure, causing an explosion and/or a fire (Brandt & Garche, 2019).

As discussed in the previous section, EV packs are designed with a BMS to control for short circuits, high temperatures and other causes of thermal runaway. There are also fuses and other safety mechanisms which are activated in the event of abuse, that is, a car accident (Brandt & Garche, 2019). Nevertheless, for recycling, regardless of whether the process is pyro or hydrometallurgical, a battery pack must be dismantled to a lower voltage and capacity by disconnecting the modules in series and parallel. Dismantling the battery pack reduces the risk of self-ignition or fire within the smelting and crushing processes. Today, in industry, dismantling is conducted manually. This procedure poses severe injury and loss of life risks due to the electrical as well as thermal, chemical and kinetic hazards. Due to the vast variety of EV pack designs available on the market, it is difficult to automate the disassembly process (Kwade & Diekmann, 2018).

2.4 Deep Discharging

Battery packs are deep discharged to lower the electrical risk. Deep discharging begins at 2.5V per cell. It has been observed that a cell at 2.5V, SOC 0%, is too high of a voltage for safe crushing since the potential between the anode and cathode is high enough to cause thermal runaway or sparking should they meet during crushing (Kwade & Diekmann, 2018). Although somewhat less hazardous, thermal runaway still occurs in cells with an SOC of 0% (Perea, et al., 2018). Below 2.5V, the cell has little capacitance left and can supply little current. Therefore, it will quickly drop to a lower voltage (see Figure 2, rightmost section).

Deep-discharging to between 1V and 0V causes an electrochemically driven, irreversible, solid-state amorphization of the crystals of the cathode active material, essentially destroying it (Shu, et al., 2012) (Ellis, 2019). During discharging, the batteries swell due to hydrogen, carbon dioxide, carbon monoxide and methane gas formation. Furthermore, as the battery continues to attempt to give more electrons to the anode, the copper anode dissolves and becomes a copper ion, potentially allowing for short circuits within the cell (Li, Gao, & Zhang, 2008). Some experts argue that these effects pose no significant safety risk particularly if the discharge is done at a low enough coulombic rate to avoid heating the cell. Additionally, the destruction of the cathode active material may not be relevant, depending on the recovery requirements of the recycling process (Sonoc, Jeswiet, & Soo, 2015). Deep discharging can be done prior to or post disassembly. Since disassembly is conducted manually, discharging prior to disassembly is the safest for the user (Kwade & Diekmann, 2018).

The standard technique for discharging a battery is electrically using static or dynamic resistance. This resistance is typically in the form of an electronic load which can be applied to a source to discharge it. The device consists of a resistor or a group of resistors, and an electronic control system (Maxey, 2019). With this device, a constant current (CC), constant resistance (CR), constant voltage (CV) or constant power (CP) can be set to discharge the battery (Kwade & Diekmann, 2018).

Typical load banks electronic loads discharge a battery using an ohmic resistance where the energy is dissipated as heat. Modern electronic loads include a 'regenerative' feature with an AC/DC inverter so the energy from the battery can be recovered as alternating current. This process is 80-94.5% efficient, therefore the energy of the battery packs arriving at a recycling facility could be recovered for further use (see Figure 5). 'Regenerative' load banks are more expensive than conventional ones but have a return on investment of 3 years (Turner, 2016). However, the efficiency is highest with high power batteries in their high-power range. The lower the power of the battery, the lower the 'regeneration'. (Poulson, 2019) (ITECH). In the deep discharged range (2.5-0V per cell), little to no energy recovery would be possible (Patulny, 2019).

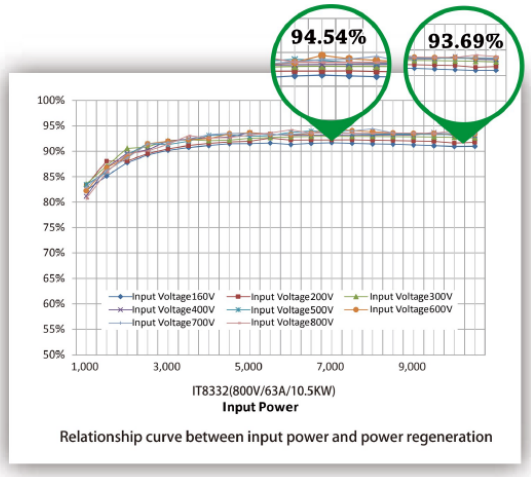

Figure 5: showing efficiency of regeneration at various power levels (ITECH)

Electronic load technology is widely used in industry to test batteries and data banks. It is a proven and commercially available technology (Kwade & Diekmann, 2018). The connection of the battery pack to the electronic load is done with electrical cables and is not typically automated. The vast variety of battery pack designs makes automating the process complex. Additionally, information about the state of health, capacitance, state of charge of the batteries and the battery's allowed voltage and current range must be known prior to discharging to ensure that the process is conducted safely. This criterion also varies by manufacturer and model and would require access to the BMS. As a result, a large volume of batteries shipped to a facility must first be sorted and information about the make and model gathered before the battery can be connected to the electronic load (Kwade & Diekmann, 2018). As discussed in the safety

section, connecting the discharging equipment to the battery pack manually can cause severe injury or loss of life and should be avoided.

2.5 Voltage Relaxation

With the issue of active material and copper degradation in mind, it would be easy to assume that discharging to 1V would be the ideal stopping point for a cell. However, there is the challenge of voltage relaxation. When a cell is deeply discharged to 0V it will rapidly return to 2.5V after a rest period (see Figure 6) (Kwade & Diekmann, 2018).

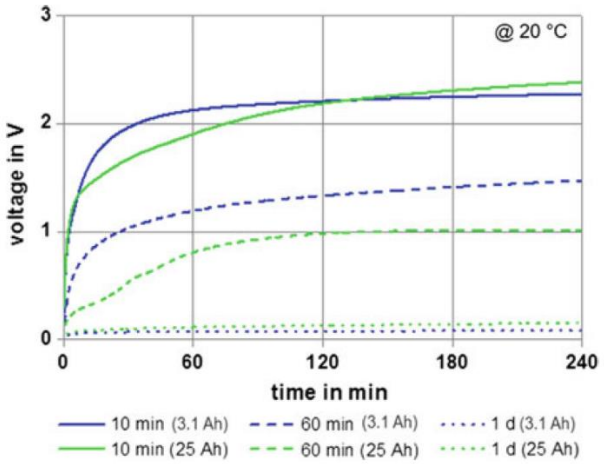

Figure 6: showing voltage relaxation curves for cells of differing capacities after differing short circuiting periods (Kwade & Diekmann, 2018)

Voltage rebound, also known as 'voltage relaxation' or 'recovery effect' is a phenomenon observed in batteries where the available energy at a given time is smaller than the sum of energies consumed and charged. That is, in the case of discharging, the energy demanded by the load is greater than the battery can momentarily provide due to the slower rate of the chemical reactions happening within it. Energy is consumed from the edge of the battery, while the total charge is spread across the entire battery. So, while the chemical reactions take place in the battery it appears, to the load device, that all the energy within the battery has been consumed. Minutes to hours later, when the battery is tested, the voltage of the battery can be 2.5V or more, despite appearing to be far below that level, in the moment of discharge (Boker , Henzinger, & Radhakrishna, 2014). The concept of voltage relaxation is illustrated below using the concept of a gas tank, where the tank is the cell, the gas is the electrons and the outflow of gas is the discharging of the cell (see Figure 7).

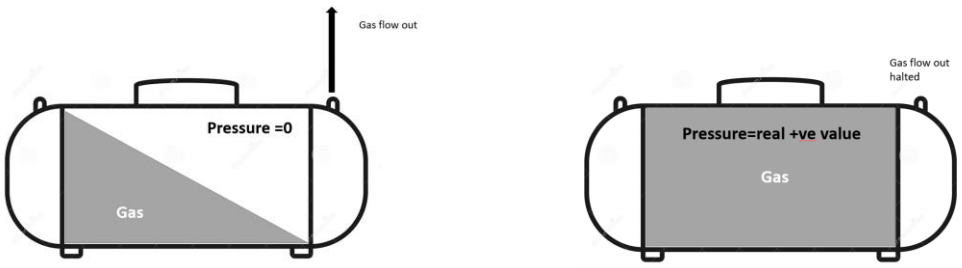

Figure 7: showing (a) what happens inside a gas tank while the gas is being rapidly depleted from one side. To the discharging device, it appears that the gas has been depleted. (b) equilibration by diffusion of the gas inside the gas tank after depletion has stopped. To the discharging device it would appear that the gas volume has 'recovered'.

In the case of recycling, if a battery is discharged too rapidly, it can momentarily appear that the battery is at 0V. The unknowing user could place the cell in the crusher, only to watch in horror as self-ignition occurs due to the voltage rebound in the period between measurement and crushing. Short circuiting is the only

means by which to ensure that the battery is at and remains below 2.5V (Kwade & Diekmann, 2018). A short circuit is a low resistance connection between the two oppositely charged electrical poles. Following the rules of Ohm's Law, this low resistance causes a high current flow, known as a 'short' (Skorucak, n.d.). The length of the short circuit is related to the rate of rebound with very long short circuits of 24 hours leading to a rebound to a lower potential than 2.5V (see Figure 6). However, rapid short circuits, that is, applying too high of a current at once, can cause temperature rise and destroy the Lithium and Copper in ways that make then unrecoverable during recycling (Kwade & Diekmann, 2018).

Qian et al have hypothesized that voltage relaxation curves can be used to determine the state of health of a cell, proving not only their commonality but also their usefulness for recycling since a lack of voltage relaxation likely signifies a critical issue within the cell (Qian, et al., 2019).

2.6 Discharging Avoidance- Inert Crushing

Inert crushing usually includes dismantling the battery pack then crushing the modules or cells in an inert environment. The environment is made inert by a flow of gas such as carbon dioxide, nitrogen or argon, or cryogenically cooling the batteries prior to crushing. The inert gas method ensures that the cell is unable to ignite, even if there is a spark, due to the lack of oxygen in the atmosphere. Cryogenically freezing the cells reduces the reactivity of Lithium by 5 or 6 orders of magnitude, so that any exothermic reactions would occur so slowly that they would not be observed. Other methods include wet crushing with a solution that will not react with the electrolyte and will convert the Lithium to an unreactive state or having a liquid spray in the presence of nitrogen while crushing (Sonoc, Jeswiet, & Soo, 2015) (World Intellectual Property Organization Patent No. WO 2015/077080 A1, 2015). Although the intention with these methods is to ensure safe crushing whilst avoiding the discharging step, some of these methods, for example inert gas crushing, are still preceded by deep discharging or consider discharging 'optional' (Archier, 2019) (United States of America Patent No. US005888463A, 1999).

Inert crushing methods can also prove costly. 1.13kg of batteries requires 2 hours of liquid nitrogen flow in order to arrive at cryogenic temperatures for crushing (United States of America Patent No. US005888463A, 1999). The flow of 'inert' gases for crushing must be under precise control since the oxygen or moisture within the casing of the cells or modules could trigger a fire (United States of America Patent No. US 207/0196725 A1, 2007). In the wet crushing methods, a high volume of waste water must be treated post crushing, which is an energy intensive process (Kwade & Diekmann, 2018).

In industry, deep discharging and inert crushing are typically coupled due to the high energy content of EV batteries. Even if the electrical hazard from the cells is minimized by deep discharging, the flammable components within the electrolyte could be ignited by even a small spark (Kwade & Diekmann, 2018).

Thermal pre-treatment of the batteries has also been explored. In this method the batteries are heated until the casing splits, the anode and cathode materials are deactivated and the electrolyte evaporates. Temperatures must arrive at 300ºC either by solely heating or with the addition of pressure. By either mechanism the process is energy intensive and releases fine particulates (Kondas, Jandova, & Nemeckova, 2006), (Kwade & Diekmann, 2018).

2.7 Unconventional Discharging Options

The methods discussed in this section were found in literature and have only been discussed in the laboratory scale (see Figure 8).

Salt Solution

Method:

The battery pack is submerged and short-circuited in solution with the salt acting as an electrolyte.

Equipment Required:

- Salt Solution Bath

Metal Powder

Method:

The battery pack is short-circuited using the metal powder with water as a thermal buffer.

Equipment Required:

- Metal Powder
- Cooling Water

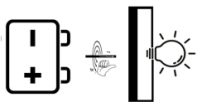

Inductive

Method:

The battery pack is electrically discharged wirelessly.

Equipment Required:

- Load Bank
- Connection to Battery
- Rectifier/Oscillator

Figure 8: showing summary of the unconventional methods found in literature

2.7.1 Salt Solution

Salt solution discharge is the method of submerging a cell in a salt solution for up to 24hours (see Figure 9). In this process, the dissolved salt acts as an electrolyte undergoing electrolysis, conducting electrons between the poles in a slow short circuit (Ojanen, Lundstrom, Santasalo-Aarnio, & Serna-Guerrero, 2018), (Sonoc, Jeswiet, & Soo, 2015). This method has been discussed extensively in literature and has generally been accepted as viable. However, few sources cite the process in depth; discussing the mechanism or the state of the cell post submersion (Ojanen, Lundstrom, Santasalo-Aarnio, & Serna-Guerrero, 2018). These sources typically state submerging the cell in 5 wt% NaCl for up to 24hours (Li, Wang, & Xu, 2016), (Xiao, Jia, & Xu, 2017). However, there are an almost equal number of sources citing corrosion of the cell casing using the same method (Ojanen, Lundstrom, Santasalo-Aarnio, & Serna-Guerrero, 2018), (Shaw-Stewart, et al., 2019). Corrosion of the cell casing causes leakage of the active materials and electrolyte, thereby releasing toxic substances or allowing self-ignition of the battery. Furthermore, submerging high voltage battery packs or modules in salt water can cause arcing and a resultant fire (Xu, et al., 2017).

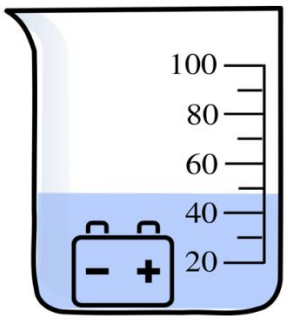

Figure 9: showing salt solution discharge method with a cell wholly submerged in solution

More recently, other salts have been attempted in the hopes that they will prove less corrosive and still sufficiently discharge the battery. Shaw-Stewart tested a host of sodium, potassium and ammonium salts, finding several that were able to discharge the cell without significant corrosion. Of his list, he recommended: Na_2CO_3, K_2CO_3, $NaHCO_3$, $NaNO_2$, NH_4OH for further testing (Shaw-Stewart, et al., 2019), (Shaw-Stewart J. , 2019). Ojanen et al. attempted another method, whereby the cell was not submerged in solution but a platinum leads connected to the poles of the cell and submerged (see Figure 10). This set up was intended to avoid corrosion of the cell but maintain the efficacy of the salt discharge (Ojanen, Lundstrom, Santasalo-Aarnio, & Serna-Guerrero, 2018). Ojanen et al. suggested $FeSO_4$, $ZnSO_4$ and Na_2SO_4 as successful salt options.

Both Ojanen et al. and Shaw-Stewart observed a significant limitation for this method, the batteries were unable to discharge beyond 1.5V, the limit for water splitting. The two exceptions they highlighted were $NaNO_2$ and $FeSO_4$ respectively, though no clear reasons were given for this (Shaw-Stewart J. , 2019) (Ojanen, Lundstrom, Santasalo-Aarnio, & Serna-Guerrero, 2018). Water splitting, that is, the process of water breaking down to hydrogen and oxygen, occurs at 1.23V theoretically (Zumdahl & Zumdahl, 2000). However, real life resistances force this limit to approximately 1.5V.

Ojanen et al. also explored the concept of cathodic protection (see Figure 10). This process involves the addition of a more corrosion susceptible metallic element into the system. By doing so, the metallic element should preferentially corrode over the cell terminals or the platinum wire. In the set-up, the platinum wires to the cell were submerged in a salt solution and then connected to either side of the powder. The addition of this metallic element dropped the discharge time to a few minutes, the batteries were discharged to 0V and some corrosion of the metallic element was seen (Ojanen, Lundstrom, Santasalo-Aarnio, & Serna-Guerrero, 2018).

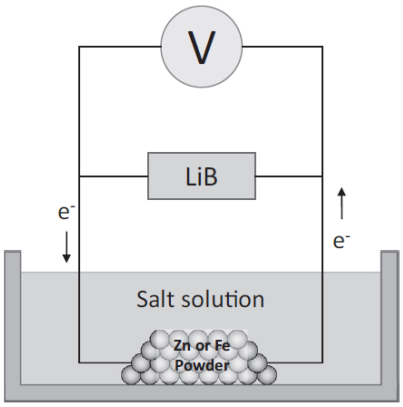

Figure 10: showing cathodic protection method used by Ojanen et al. (Ojanen, Lundstrom, Santasalo-Aarnio, & Serna-Guerrero, 2018)

Other than water splitting, the primary disadvantage of this method is that if an entire EV pack is placed into the solution for discharging, there is the risk of high voltage arcing and significantly high temperature rise, potentially posing significant damage to the recycling facility (Ellis, 2019). Therefore, if the current at the positive terminal cannot be kept below 90,000A/m^2, dismantling would have to occur before discharging (Xu, et al., 2017).

Additionally, information about the waste stream is necessary. Li et al. conducted tests on the waste stream using NaCl. Since NaCl is corrosive, the stream contained dissolved casing metal. The most alarming discovery was the presence of metals from the cathode active material (Li, Wang, & Xu, 2016). Less corrosive salts may not pose the problem of dissolution of the active material but may still contain traces of the casing metals and other products of the electrolysis. The treatment required for the waste solution requires further investigation.

2.7.2 Metal Powder Discharge

A lesser known alternative is the method of placing the cells in a stainless-steel container with water and a metal powder (see Figure 11). As in the salt solution method, little is known about the mechanism of the discharge and little is said about the state of the cell after the discharge is completed (Nan, Han, & Zuo, 2005), (Gratz, Sa, Apelian, & Wang, 2014).

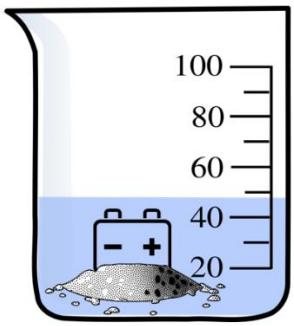

Figure 11: showing metal powder discharge method

The water is meant to act as a buffer to thermal runaway while the metal acts as a conductive, low resistance path for short circuiting. According to Nan et al., after half an hour of short circuiting, the batteries were 'completely discharged'. Gratz et al. repeated the process several years later. After four hours of short circuiting, the voltage of the cells was below 2V, after which the batteries were sent for crushing (Gratz, Sa, Apelian, & Wang, 2014). Wang conducted a similar experiment instead using graphite as a thermal buffer. However, the temperature of the cell increased rapidly, suggesting that graphite is not the most efficient thermal buffer in this procedure (Wang H. , 2013). Although, short circuiting is an efficient method for ensuring the batteries are sufficiently deep discharged, the process, if not controlled, can artificially heat the battery, causing thermal runaway and self-ignition (Larsson, 2014).

The risk of arcing in this method is greater than in the salt solution method since the conductivity of the metal is higher. If an entire EV pack is placed into the metal-water bath for discharging, there is the risk of high voltage arcing and significantly high temperature rise, potentially posing significant damage to the recycling facility (Ellis, 2019).

2.7.3 Inductive (Dis)charging

The concept of inductive discharging for batteries was borne by the idea of having a wireless resistive discharge so that the manual component of connecting the batteries could be eliminated (see Figure 12). Inductive charging has gained notoriety of late, as phone and tablet companies attempt to find alternate ways for users to charge their devices (Battery University, n.d.). Typically, only wireless charging is discussed in literature, however, the feasibility of bidirectional chargers has been explored by Honda and WiTricity. From their research, it is also possible to discharge a battery using this method in a vehicle-to-grid (V2G) operation (Tachikawa, Kesler, & Atasoy, 2018).

Figure 12: showing inductive charging an EV (WiTricity, n.d.)

The process of inductive charging is the similar to that of a transformer where a coil with a current passing through it, thereby creating a magnetic field, induces a current in another coil aligned with the magnetic field of the first. In the case of inductive charging, there is no metal connecting the coils to "allow" the transfer of the magnetic field, instead the two coils are magnetically coupled, through air, using an oscillator and a rectifier in resonance. Once the coils are in resonance, the current from the source is induced in the load and the device is charged. The shorter the distance between the two load and the source, the stronger the current (Andersson & Oddeby, 2018).

The process can be used at high and low power levels and is being used in Sweden to charge electric buses in a project called Primove. In Primove, the process inducts 200kW of power to an electric bus in approximately 7 minutes (Mannheim Transportation, 2016). However, for this method to work, a pad equipped with a coil and power electronics must be connected to the terminals of the battery. In order to avoid the manual step of connecting the pad to the terminals of the battery, this device should be installed in the battery by the manufacturer prior to installation in the vehicle (Wambsganss, 2019).

A receiving slab or pad must also be installed at the recycling facility. This receiver should be equipped with the secondary coil, power electronics and safety sensors so that the charging/discharging process does not destroy the battery and to protect the user since the magnetic field exposure is higher than is allowed by international regulations. The system of discharging the battery would be equivalent to that of the resistive method, so the same procedure used for resistive discharge could be transferred to the inductive discharge method. However, currently, inductive charging pads are not regularly installed in EVs except in projects such as Primove (Wambsganss, 2019) (Mannheim Transportation, 2016).

3 Methodology

3.1 Experimental for Rapid Resistive Discharge to 0V

For proof of concept, tests were conducted on cylindrical cells with a relatively low capacitance. This was done to minimize the risk of fire or explosion during testing. The batteries were 21700, cylindrical, lithium-ion cells: 3.25Ah, 4.2V max voltage, 3.6 nominal voltage.

The methodology was as follows:

1. Fit 4 cells with leads and connect them to the battery test system (Lanhe CT2001A) with a programmable user interface (LAND Battery Testing System- Data Processing Software V5.9H).
2. Discharge the batteries from 3.5V to -0.5V with a current of 1.625A.
3. Allow programme to stop as soon as -0.5V is recorded.
4. Confirm voltage of cells with multimeter (APPA 73 True RMS Multimeter) 2 hours post discharge

3.2 Experimental for Slow Resistive Discharge to 0V

For proof of concept, tests were conducted on cylindrical cells with a relatively low capacitance. This was done to minimize the risk of fire or explosion during testing. The batteries were 21700, cylindrical, lithium-ion cells: 3.25Ah, 4.2V max voltage, 3.6 nominal voltage.

The methodology was as follows:

1. Fit 4 cells with leads and connect them to the battery test system (Lanhe CT2001A) with a programmable user interface (LAND Battery Testing System- Data Processing Software V5.9H).
2. Discharge the cells from 2.8V to -0.5V with a constant current of 0.2A.
3. If discharge time will be less than 120 minutes, change current to 0.05A
4. If discharge time will be less than 120 minutes, change current to 0.01A
5. Allow programme to stop as soon as -0.2V is recorded.
6. Confirm voltage of cells with the multimeter (APPA 73 True RMS Multimeter) 2 hours post discharge

3.3 Experimental for Salt Solution Discharge

From the solutions tested by Shaw-Stewart and Ojanen et al. and the relevant results, the following solutions were chosen:

1. Na_2SO_4 (Honeywell, 99.0%)
2. $FeSO_4$ (as heptahydrate, Merck Millipore, 99%)
3. $NaHCO_3$ (Merck Millipore, 99%)
4. Na_2CO_3 (VWR Chemicals, 99.8%)
5. $NaNO_2$ (Merck Millipore, 98%)
6. $NaNO_3$ (Merck Millipore, 99%)
7. K_2CO_3 (Merck Millipore, 99%)

For proof of concept, tests were conducted on cylindrical cells with a relatively low capacitance. This was done to minimize the risk of fire or explosion during testing. The batteries were 21700, cylindrical, lithium-ion cells: 3.25Ah, 4.2V max voltage, 3.6 nominal voltage. The experimental procedure was as such:

1. Prepare 1000mL of 5wt% solution with distilled water.
2. Weigh the cell (VWR Collection, LP Series) and test the voltage of the cell using the multimeter (APPA 73 True RMS Multimeter).
3. Test temperature, conductivity and pH of solution using the pH meter (Orion Star A211).

4. Place cell in solution with tongs
5. After 1 hour, remove the battery from solution with tongs, check for corrosion, dry, measure weight and voltage. While battery is out of solution, test pH, conductivity and temperature of the solution. If battery is visibly corroded, terminate experiment. If not, replace the battery in solution.
6. Repeat step 5 every hour for 6-8 hours. Then, leave the cell in solution for a total of 24 hours, remove the cell from solution with tongs, check for corrosion, dry, measure weight and voltage. Test pH, conductivity and temperature of the solution. Leave cell in ambient, do not replace in solution.
7. After 1 hour, test the voltage of the cell, if less than 2.5V test the voltage every hour until 2.5V is reached or greater than 7 hours has elapsed.

3.4 Experimental for Salt Solution Discharge Tests under Various Conditions

Based on the results of 3.3, the following laboratory tests was suggested. The following solutions were tested for the efficacy of the salt solution discharge in the following conditions:

Solutions:

1. $NaHCO_3$ (Merck Millipore, 99%)
2. Na_2CO_3 (VWR Chemicals, 99.8%)
3. $NaNO_2$ (Merck Millipore, 98%)
4. $NaNO_3$ (Merck Millipore, 99%)
5. K_2CO_3 (Merck Millipore, 99%)

Conditions:

1. 10% weight
2. 5% weight at 40-50°C
3. 10% weight at 40-50°C (Na_2CO_3 and K_2CO_3 only)

For proof of concept, tests were conducted on cylindrical cells with a relatively low capacitance. This was done to minimize the risk of fire or explosion during testing. The batteries were 21700, cylindrical, lithium-ion cells: 3.25Ah, 4.2V max voltage, 3.6 nominal voltage.

1. Prepare 1000mL of 5wt% or 10% solution in distilled water
2. For the heated solution, prepare a water bath (Lauda Eco Gold) at 50ºC.
3. Weigh the cell (VWR Collection, LP Series) and test the voltage using the multimeter (APPA 73 True RMS Multimeter).
4. Test temperature, conductivity and pH of solution using the pH meter (Orion Star A211).
5. Place battery in solution with tongs
6. After 1 hour, remove the battery from solution with tongs, check for corrosion, dry, measure weight and voltage. While battery is out of solution, test pH, conductivity and temperature of the solution. If battery is visibly corroded, terminate experiment. If not, replace the battery in solution.
7. Repeat step 6 every hour for 6-8 hours. Then, leave the solution for a total of 24 hours, remove the battery from solution with tongs, check for corrosion, dry, measure weight and voltage. Test pH, conductivity and temperature of the solution. Leave battery in ambient, do not replace in solution.

8. After 1 hour, test the voltage of the battery, if less than 2.5V test the voltage every hour until 2.5V is reached or greater than 7 hours has elapsed.

3.5 Experimental for Metal Powder Discharge

From the tests done by Nan et al. and Gratz et al., the following metals were chosen:

1. Steel chips (Office Depot Chrome Staples or Rapid Super Strong 9/12 Staples)

The following solutions were chosen:

1. Distilled Water
2. $NaHCO_3$ (Merck Millipore, 99%)
3. Na_2CO_3 (VWR Chemicals, 99.8%)
4. $NaNO_2$ (Merck Millipore, 98%)
5. $NaNO_3$ (Merck Millipore, 99%)
6. K_2CO_3 (Merck Millipore, 99%)

For proof of concept, tests were conducted on cylindrical cells with a relatively low capacitance. This was done to minimize the risk of fire or explosion during testing. The batteries were 21700, cylindrical, lithium-ion cells: 3.25Ah, 4.2V max voltage, 3.6 nominal voltage. The experimental procedure was as such:

1. Prepare metal in 1000mL of distilled water
2. Weigh the cell (VWR Collection, LP Series) and test the voltage using the multimeter (APPA 73 True RMS Multimeter).
3. Test temperature, conductivity and pH of solution using the pH meter (Orion Star A211).
4. Place battery in plastic container with tongs
5. After 1 hour, remove the battery from solution with tongs, check for corrosion, dry, measure weight and voltage. While battery is out of solution, test pH, conductivity and temperature of the solution. If battery is visibly corroded, terminate experiment. If not, replace the battery in solution.
6. Repeat step 5 every hour for 6-8 hours. Then, leave the solution for a total of 24 hours, remove the battery from solution with tongs, check for corrosion, dry, measure weight and voltage. Test pH, conductivity and temperature of the solution. Leave battery in ambient, do not replace in solution.
7. After 1 hour, test the voltage of the battery, if less than 2.5V test the voltage every hour until 2.5V is reached or greater than 7 hours has elapsed.

3.5.1 Preparation of Steel in the form of Staples

1. Place 5-6 rows of staples (Office Depot Chrome Staples or Rapid Super strong 9/12 Staples) into a beaker
2. Add acetone (Honeywell, 99.0%) and mix until the binder has dissolved and all the staples are separated
3. Rinse with distilled water
4. Fill beaker with 200 mL of distilled water
5. Add 50-100mL of 30% HCl (Merck Millipore)
6. Leave for 2-3 minutes
7. Decant staples
8. Rinse with distilled water

4 Results and Discussion

For proof of concept, the electronic load discharge, salt solution discharge and metal powder discharge tests were conducted according to the methodologies listed in the previous section. The intention was to understand the processes to determine their efficacy for industrial use and if/how they could be improved. The tests were conducted on cylindrical cells with a relatively low capacitance to minimize the risk of fire or explosion during testing. Successful tests could slowly be upscaled to cells with higher capacitances until entire battery packs are shown to discharge effectively by any of these methods. Since little information is available in literature on discharging EV batteries on a module or pack scale, interviews were conducted with industry professionals to understand the methods. From those discussions, it was clear than no one method exists and there is room for improvement in this area. Improvement would take the form of several key performance indicators (KPIs). The discharge methods chosen were compared with the KPIs to determine the areas for development (see Table 1). It was decided that inductive discharge would be too large of a scope for the thesis and was only evaluated theoretically with discussions with industry professionals:

1. A process that is 'safe' that is, reduces the risk to the facility by minimizing the fire or explosion hazard
2. A process that is 'safe' that is, minimizes or eliminates human interaction with the battery pack
3. A process that is 'safe' that is, voltage rebound of the cell is limited to no greater than 0.5V.
4. A process that is 'rapid', that is, ensures that the discharging process does not become a bottleneck in the recycling process
5. A process that is 'sustainable' that is, has no polluting fluid waste streams
6. A process that is 'feasible' that is, is cost efficient

Table 1: showing the four explored methods compared with the key performance indicators based on literature and observation. Green means that the KPI is met, orange means that the KPI may be met dependent on various factors, red means the KPI is not met.

	Minimizes Fire or Explosion Hazard	**Minimizes Human Interaction**	**Voltage Rebound Limited to 0.5V**	**Rapid (4hrs or less)**	**Sustainable (non-polluting)**	**Cost Efficient**
Electronic Load						
Salt Solution						
Metal Powder						
Inductive						

0.5V as opposed to 0.0V was chosen to be the upper limit for crushing. Several cells discharged to 0.5V were opened and no sparks or other fire hazards were observed. Additionally, as will be seen in later sections, 0.0V is not a realistic value due to the natural potential between the electrodes. If 0.0V is reached, that would mean the separator has become destroyed and the anode and cathode are in contact, posing a dangerous short-circuiting risk. Additionally, due to the research by Qian et al, voltage rebound was considered a positive scale by which to measure the state of the health of the cell. If voltage rebound is not observed, even if only to 0.5V, then it could be assumed that the cell was damaged by the discharge method (Qian, et al., 2019).

4.1 Resistive discharge with an Electronic Load

Although the resistive discharge with an electronic load method is the most conventional deep discharge method available in industry, no procedure has been discussed or been made publicly available. The intention with this test was to understand how long would be required to effectively discharge a cell to or below 0.5V. This value would be used as a benchmark for the unconventional methods. If the

unconventional methods could pose a shorter discharge time and/or prove easier to automate, then they could be considered for industrial applications.

In the fast discharge programme, -0.5V was chosen as the lower value for discharging since Kwade et al., discussed a pole reversal at 0V. Beyond 0V, the anode and cathode trade polarity. In this process, the cell can heat up to 50 °C in 15 minutes, proving that a pole reversal may be hazardous. That being said, Kwade et al. observed that after post pole reversal, the cell voltage returned to 0V and did not rise (Kwade & Diekmann, 2018). Therefore, if the cell could be rapidly discharged to pole reversal, not rebound above 0V and not overheat, then the method would prove effective.

To prove this, the cell was rapidly discharged from 3.5V to -0.5Vat 0.5C (1625 mA) in just under 30 minutes (see Figure 13). Two hours after the completion of the discharge, the voltage of the cell was ~2.7V. As a result, it was confirmed that discharging to -0.5V at 0.5C does not allow for pole reversal since rebound to above 2.5V occurred.

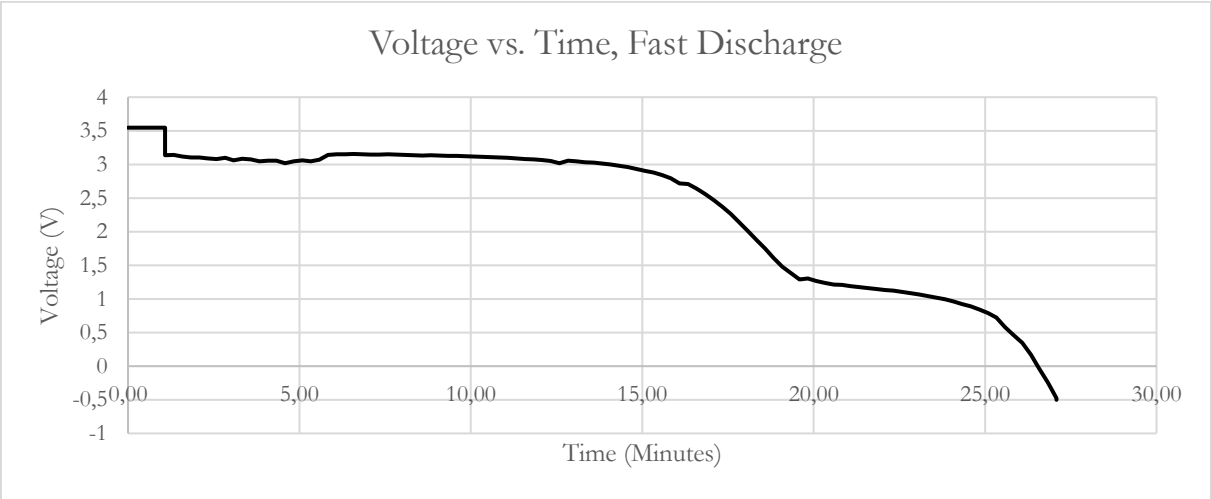

Figure 13: Showing fast resistive discharge curve

A second attempt was made, this time, the process was repeated with the current at 0.2A, then lowered to 0.05A at approximately minute 10, then again to 0.010A at approximately minute 50 (see Figure 14). Due to concerns about overheating, since a slow discharge would maximise the time spent below 0.0V, the lower limit in this case was changed to -0.2V.

Voltage rebound can be observed both times the voltage was changed. The total discharge time was just over 4 hours. The following day the batteries were tested and the voltage found to be ~0.5V. Weeks later, the voltage of the cells was still ~0.5V. Since voltage rebound was above 0.0V, it was assumed that there was no pole reversal. However, since the cells remained at 0.5V for several weeks, then discharging without pole reversal and the risk of overheating was considered viable. The minimum reference discharge time was set at 4 hours as a result of these experiments.

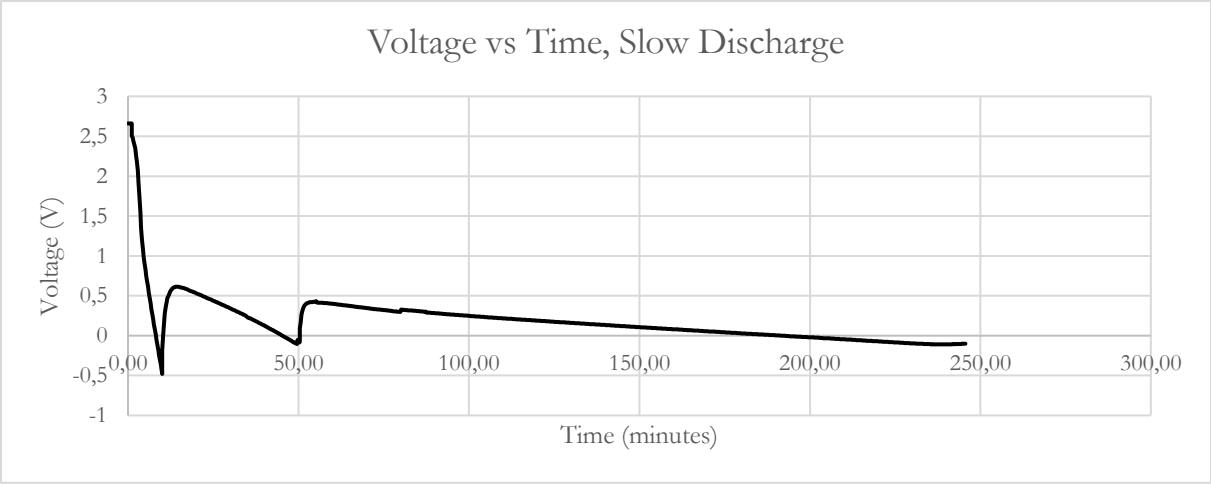

Figure 14: showing slow resistive discharge curve

4.2 Salt solution Discharge

Prior to testing this method, it was known that the discharge time would be longer than 4 hours and that the lower limit would be 1.5V (Shaw-Stewart, et al., 2019) (Ojanen, Lundstrom, Santasalo-Aarnio, & Serna-Guerrero, 2018). However, the intention with these experiments was first to find solution(s) that did not corrode the cell casing, then to put the solution(s) through various conditions to find if one could overcome the 1.5V barrier or have a discharge time equivalent to or shorter than 4 hours. As discussed in the background, corrosion of the casing could cause leakage of the electrolyte and the active materials, producing hydrogen fluoride, flames or an explosion.

Should a suitable salt be found, the salt solution discharge method would be easier to automate than the resistive method since whole battery packs could be placed into solution without concern about the connection to the terminals. The primary concern with submerging whole battery packs into solution would be arcing. Arcing is the discharge of electricity between electrodes in a gas or vapour which causes a breakdown of the chemical composition of the gas (Compton, 1927). Due to the energy expelled during an arc, arcing fuses the positive terminal releasing the electrolyte, which, when ignited due to the arc, burns at the surface of the solution. In the case where whole or simulated EV packs were submerged in 2.4 wt% sodium chloride solution, arcing was observed at 250V which is the lower limit for an HEV battery (Xu, et al., 2017).

The positive terminal has a higher potential than the negative and is the site of rapid electrolysis (Shaw-Stewart J. , 2019). At high voltages (above 60V), arcing occurs at a current density of 90,000 A/m^2 in 3.5wt% NaCl (Xu, et al., 2017). The cells tested in this thesis had a positive terminal area of 0.64cm^2, therefore the arc current would be 5.76A in 3.5wt% sodium chloride solution. Since sodium chloride is a highly conductive solution (~50mS/cm), solutions with a lower conductivity should have a higher arc current allowing for higher voltage batteries to be submerged and safely discharged (Lenntech, n.d.). Since arcing is caused by the breakdown of gases at the positive terminal, solutions that do not produce gas bubbles should be preferentially chosen or, if unavoidable, the solutions should be stirred to limit the number of bubbles around the positive terminal (Xu, et al., 2017).

The larger the 'contact area', in this case the size of the positive terminal, the higher the arc current (Xu, et al., 2017). For a battery pack or module, the terminal size would be far larger than for a cylindrical cell, therefore, the arc current would be higher, again allowing for higher voltage battery packs to be safely submerged. When envisioning modules or battery packs a positive terminal area of 6.25cm^2 and a resultant arc current of 56.25A was chosen.

Returning to the experiments undertaken in this thesis, since no tests were conducted to determine the composition of the gases or liquids during or after the experiment, half reactions at the positive terminal

(cathode) and negative terminal (anode) have been proposed for each salt (Shaw-Stewart, et al., 2019) (Vanysek, 2010) (Shipley, 1934). As will be discussed, electrolysis in solution is controlled by a multitude of factors including (EasyChem, n.d.):

- Increased current
- Increased voltage
- Increased concentration of ions in electrolyte (salt solution)
- Increased surface area of electrodes
- Decreased distance between electrodes
- Inert electrode to active electrode

Since the voltage, surface area, distance between electrodes and composition of the cells is held constant, the factors influencing the discharge mechanism in the solutions would be increased current and increased concentration of ions. To quantify the effect of these factors, ionic strength, that is, the total ion concentration in solution has been calculated according to the equation (Haynes, 2010):

Equation 1- ionic strength

$$\mu = \frac{1}{2}\sum_{i=1}^{n} []_i Z_i^2$$

μ- ionic strength

[]- concentration of ions

Z-ionic charge

The standard theoretical conductivity of each solution was used to determine the probable current in solution to further understand the rate of discharge (Haynes, 2010) (Aqion, n.d.). The current was calculated according to the equation:

Equation 2-starting current

$$I = \frac{V_{cell\_start}}{KD^{-1}}$$

I- current

K- conductivity

D- Length of the positive terminal

Finally, using the size of the positive terminal as a reference, the largest possible battery pack in terms of voltage was determined assuming a terminal size of 6.25cm² and an arc current of 56.25A according to the equation (Xu, et al., 2017):

Equation 3- maximum battery pack voltage before arcing

$$V_{battery\ pack} = (KD)^{-1} I_{arc}$$

I_{arc}- Arc current

$V_{battery\ pack}$- Maximum allowed voltage of battery pack before arcing

4.2.1 Sodium Sulphate, Na_2SO_4

Ions in solution before electrolysis:

Na_2SO_4 (s) $+2H_2O$ (l) → $2Na^+$ (aq) + SO_4^{2-} (aq) + $2H^+$ (aq) + $2OH^-$ (aq) (1)

During electrolysis

Possible reactions at the Anode:

Na^+ (aq) + e^- ⇌ Na (s)	E0= -2.71V	(2)
$2H^+$ (aq) + 2e- ⇌ H_2(g)	E0= 0.0V	(3)*

Possible reactions at the Cathode:

$2H_2O$ (l) ⇌ O_2 (g)+ $4H^+$ (aq)	E0= -1.23V	(4)*
SO_4^{2-} (aq) + $4H^+$ (aq) + $2e^-$ ⇌ H_2SO_3 (aq)+ H_2O (l)	E0= 0.172V	(5)
$2SO_4^{2-}$ (aq) + $4H^+$ (aq) + $2e^-$ ⇌ $S_2O_6^{2-}$ (aq) + H2O (l)	E0= –0.22V	(6)
SO_4^{2-} (aq) + H_2O (l) + $2e^-$ ⇌ SO_3^{2-} (aq) + $2OH^-$ (aq)	E0= –0.93V	(7)*

*denotes most likely reactions in solution

The experiment was terminated in the 6th hour due to corrosion of the positive terminal (see Figure 16 and Figure 15). This solution is not suggested for salt solution discharge at any scale since it becomes significantly corroded and further corrosion could prove hazardous.

Upon submersion, gas bubbles were produced indicating likely hydrogen and oxygen gas formation according to reactions 3 and 4. By the second hour, a yellow film began to form at the surface of the solution and some corrosion of the positive terminal became visible. By the 6th hour, the positive terminal was almost completely corroded with a black precipitate, possibly either an iron or nickel oxide, forming around the terminal. The yellow film in the solution had grown in thickness and was much closer to an orange-brown colour (see Figure 16).

The solution became more basic during the progression of the experiment going from pH 5.54 to 9.86, suggesting hydroxide formation in line with reaction 7. There was also 0.3g of loss of the cell weight. It is also likely that the oxygen produced in solution reacted with the metal of the casing likely contributing to the oxidation of the positive terminal. Secondary reactions involving the oxidised casing or the sulphite ions in solution likely caused the film at the surface of the solution.

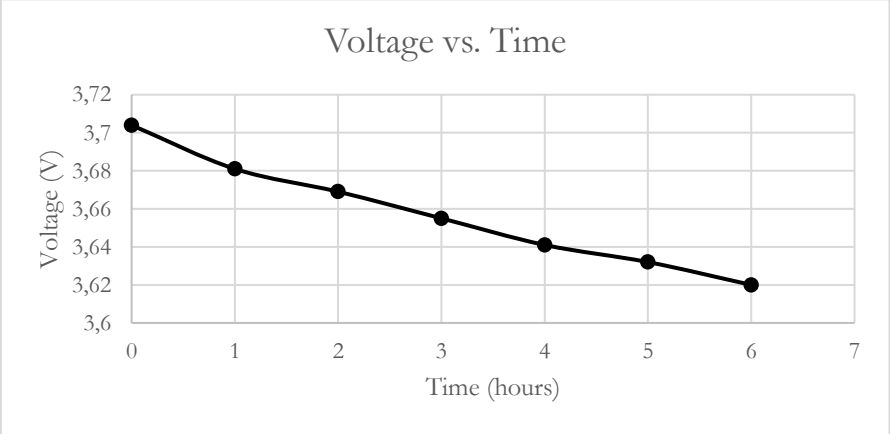

Figure 15: salt solution discharge using Na_2SO_4 solution

Figure 16: showing (a) corrosion of the casing after 6 hours, (b) orange-brown film at the surface of the solution after 6 hours

4.2.2 Iron Sulphate, $FeSO_4$

Ions in solution before electrolysis:

$FeSO_4$ (s) $+H_2O$ (1) → Fe^{2+} (aq) + SO_4^{2-} (aq) + H^+ (aq) + OH^- (aq) (8)

During electrolysis

Possible reactions at the Anode:

Fe^{2+} (aq) + $2e^-$ ⇌ Fe (s) E0= –0.447V (9)

$2H^+$ (aq) + $2e^-$ ⇌ H_2(g) E0= 0.0V (10)*

Possible reactions at the Cathode:

$2H_2O$ (l) ⇌ O_2 (g) + $4H^+$ (aq) E0= -1.23V (11)*

SO_4^{2-} (aq) + $4H^+$ (aq)+ $2e^-$ ⇌ H_2SO_3 (aq) + H_2O (l) E0= 0.172V (12)

$2SO_4^{2-}$ (aq) + $4H^+$ (aq)+ $2e^-$ ⇌ $S_2O_6^{2-}$ (aq) + H_2O (l) E0= –0.22V (13)

SO_4^{2-} (aq) + H_2O (l) + $2e^-$ ⇌ SO_3^{2-} (aq) + $2OH^-$ (aq) E0= –0.93V (14)

The experiment was terminated at hour 3 due to complete corrosion through the casing of the cell. This observation was made after the cell was removed from solution during which venting was heard and a fire became visible at the positive terminal. Less than 0.1V of discharge had been recorded in the previous hour (see Figure 17). This solution is strongly discouraged for further testing.

Bubbles were observed upon submersion. It is likely that there was oxygen and hydrogen formation according to reactions 10 and 11. The pH of the solution was 2.13 at the start of the experiment and 2.22 at the end, suggesting there was a weak acid or dilute strong acid in solution. It is likely that the acid was sulphuric acid (H_2SO_4). After the first hour of submersion, dissolution of the casing was visible around the positive terminal (see Figure 18).

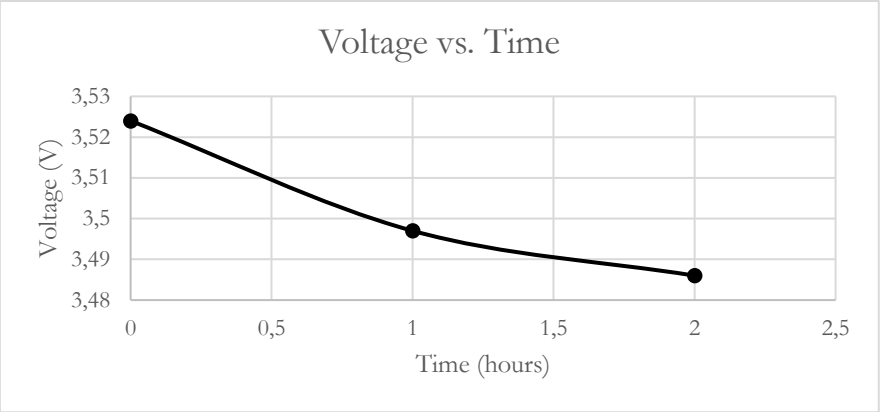

Figure 17: salt solution discharge using $FeSO_4$

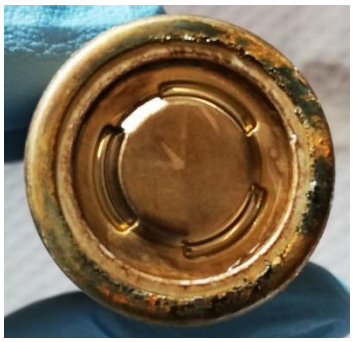

Figure 18: Corrosion of the cell casing in the 2nd hour

4.2.3 Sodium Hydrogen Carbonate, $NaHCO_3$

Ions in solution before electrolysis:

$NaHCO_3$ (s)+ H_2O (l) → Na^+ (aq) + H^+ (aq) + $HCO3^-$ (aq) + OH^- (aq) (15)

During electrolysis

Possible reactions at the Anode:

Na^+ (aq)+ e^- ⇌ Na(s) E0= -2.71V (16)

H_2O (l) + $2e^-$ ⇌ H_2 (g) + $2OH^-$ (aq) E0= -0.83V (17)*

Possible reactions at the Cathode:

$4OH^-$ (aq) ⇌ O_2 (g) + $2H_2O$ (l) + $4e^-$ E0= -0.40V (18)

4 $HCO3^-$ (aq) ⇌ $2H_2O$ (l) +$4CO_2$ (g) + O_2 (g) +$4e^-$ E0= -1.45 to -1.50 (19)*

The experiment was able to undergo 24 hours of discharging without visible corrosion (see Figure 19). Post discharge, the casing appeared completely intact and the effect of voltage rebound to 2.5V was observed. It can be seen that the rate of discharge increased with submersion time however, slows, likely becoming asymptotic, as the cell voltage approaches a limit at 1.81V. Voltage rebound is rapid, with the cell returning to 2.5V in two hours.

The solution had a pH of 7.9 at the beginning of the experiment and 8.56 at the end, suggesting negligible amounts of base formation or consumption of the acids in solution according to reaction 19. Bubble

production was observed in this solution therefore, it is likely that carbon dioxide, oxygen and hydrogen gases were formed according to reactions 17 and 19. Since the solution became slightly more basic rather than less, it is unlikely that oxygen and water formation according to equation 18 occurred even though it has a lower electrostatic potential than 19. Bubble production slowed almost to a halt at a cell voltage of ~2V, suggesting a slowing in the rate of electrolysis as the 1.81V limit is reached. It is possible that the limit is controlled by reaction 19 and not by water splitting, though further tests would need to be conducted to confirm this hypothesis. Nevertheless, this solution is strongly recommended for salt solution discharge on an industrial scale.

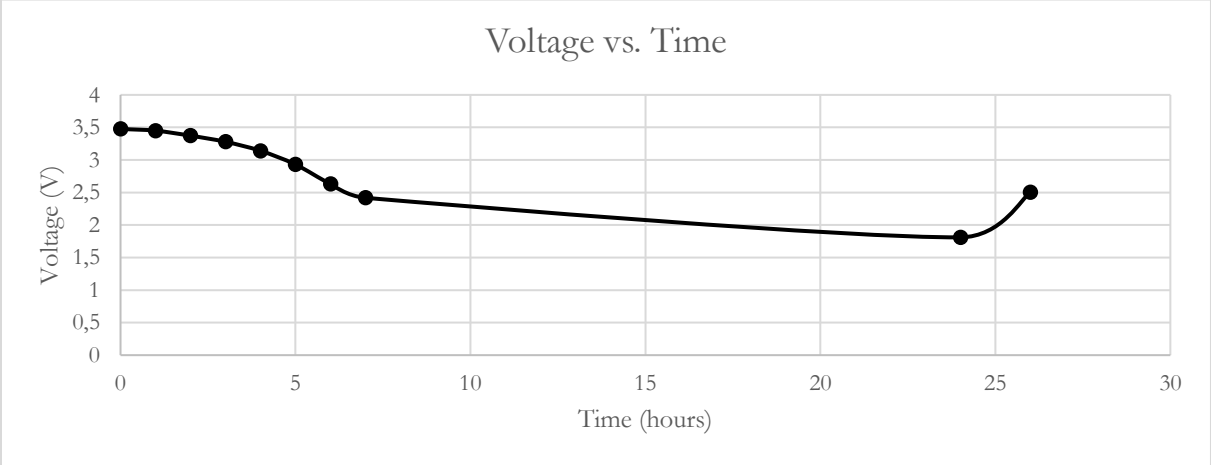

Figure 19: salt solution discharge using $NaHCO_3$

4.2.4 Sodium Carbonate, Na_2CO_3

Ions in solution before electrolysis:

Na_2CO_3 (s) + $2H_2O$ (l) → $2Na^+$ (aq) + $2H^+$ (aq) + CO_3^{2-} (aq) + $2OH^-$ (aq) (20)

During electrolysis

Possible reactions at the Anode:

Na^+ (aq) + e^- ⇌ Na(s) E0= -2.71V (21)

H_2O (l) + $2e^-$ ⇌ H_2 (g) + $2OH^-$ (aq) E0= -0.83V (22)*

Possible reactions at the Cathode:

4 OH^- (aq) ⇌ O_2 (g) + 2 H_2O (l) + $4e^-$ E0= -0.40V (23)*

$2CO_3^{2-}$ (aq) ⇌ $2CO_2$ (g) +O_2 (g) +$2e^-$ E0= -1.90 to -1.95 (24)*

The experiment was able to undergo 24 hours of discharging without visible corrosion (see Figure 20). Post discharge, the casing appeared completely intact and the effect of voltage rebound was observed for 24 hours. It can be seen that the rate of discharge is almost linear for the first six hours, meaning that there is a rapid increase in the rate of discharge during the un-tested hours (6^{th} to 24^{th} hour). A follow up test was conducted to determine when the rate of discharge changed. This test left the cell in solution overnight starting in the evening. At hour 17, the following morning, the voltage was 1.723V. It is likely, thus, that there is a turning point after hour 6 but before hour 17, where the battery is rapidly discharged. From that point, the discharge becomes asymptotic. The limit of water splitting is observed in this solution at 1.723-1.879V.

The solution had a pH of 11.14 at the beginning of the experiment and 10.97 at the end, suggesting a weak base or dilute strong base was in solution. The base was likely sodium hydroxide (NaOH). Bubble production was observed in this solution until ~2V therefore, it is likely that carbon dioxide, oxygen and hydrogen gases were formed according to reactions 22, 23 and 24. Since the solution became slightly less basic, it is possible that reaction 24 is the main reaction with secondary amounts of reaction 23 forming water and consuming the base in solution. After ~2V, reactions 23 and 24 take over, the net reaction being water splitting. Since this discharge halts at 1.723-1.879V it is likely that this is the limit of water splitting for this solution.

The voltage rebound in Na_2CO_3 is slower than in $NaHCO_3$, with the voltage arriving at 2.5V more than eight hours after removal from solution. According to work done by Qian et al., this suggests that the cell in $NaHCO_3$ was less healthy than Na_2CO_3 (Qian, et al., 2019). The cell used in Na_2CO_3 was cycled prior to testing and started at a higher voltage and capacity. It is unclear how this difference in starting condition affected the 'health' of the cell in solution. This solution is strongly recommended for salt solution discharge on an industrial scale.

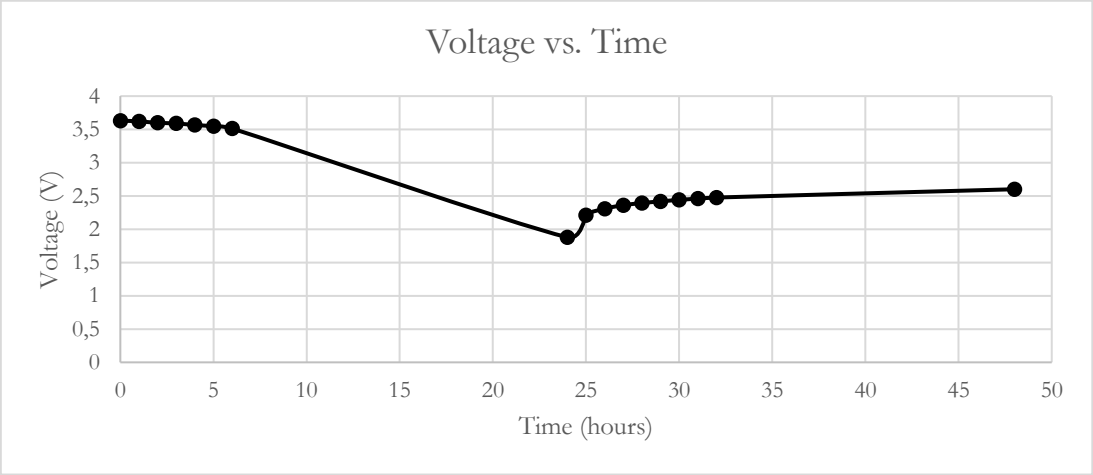

Figure 20: salt solution discharge using Na_2CO_3 solution

4.2.5 Sodium Nitrite, $NaNO_2$

Ions in solution before electrolysis:

$NaNO_2$ (s) + H_2O (l) → Na^+ (aq) + H^+ (aq) + NO_2^- (aq) + OH^- (aq) (25)

During electrolysis

Possible reactions at the Anode:

Na^+ (aq) + e^- ⇌ Na(s) E0= -2.71V (26)

H_2O (l) + $2e^-$ ⇌ H_2 (g) + $2OH^-$ (aq) E0= -0.83V (27)*

Possible reactions at the Cathode:

$4OH^-$ (aq) ⇌ O_2 (g) + $2H_2O$ (l) + $4e^-$ E0= -0.40V (28)*

NO_2^- (aq)+ H_2O (l) + e^- ⇌ NO (g) + $2OH^-$ (aq) E0= –0.46V (29)

$2NO_2^-$ (aq) + $2H_2O$ (l) + $4e^-$ ⇌ $N_2O_2^{2-}$ (aq) + $4OH^-$ (aq) E0= –0.18V (30)*

$2\ NO_2^-\ (aq) + 3H_2O\ (l) + 4e^- \rightleftharpoons N_2O\ (g) + 6OH^-\ (aq)$ E0= 0.15V (31)

The experiment was able to undergo 24 hours of discharging (see Figure 21). Post discharge, the casing appeared to have undergone uniformed corrosion with likely black nickel oxide and orange iron oxides forming on the positive electrode (see Figure 22). Additionally, blue-green crystals were formed at the positive electrode. The composition of the crystals is unkown but is thought to be a sodium salt (Shaw-Stewart J. , 2019).

As in the previous solutions, it can be seen that the rate of discharge is slow for the first six hours, meaning that there is a rapid increase in the rate of discharge during the un-tested hours. This solution approaches the limit of water splitting at 1.619V, proving that some of the resistance in solution is overcome by the ions.

The pH of this solution was 8.15 at the beginning of the experiment and 11.65 at the end. Since no gas formation was observed and the solution became basic, it is likely that reaction 30 is the predominant reaction. Oxygen formation according to reaction 28 is likely since the positive terminal becomes oxidized, therefore the oxygen is consumed by the casing metals rather than escaping as a gas. It is likely that the hydrogen gas is also consumed rather than escaping as a gas. Therefore, although the limit of water splitting is observed, it is lower than that of other solutions due to the competing reaction 30.

The voltage rebound in this solution is at more or less the same rate as Na_2CO_3, with the voltage arriving at 2.5V more than eight hours after removal from solution. This cell was also cycled prior to testing. $NaNO_2$ could be a likely candidate for salt solution discharge on an industrial scale however, much research would need to be done into the precipitates forming in solution and the state of the waste stream since some corrosion of the casing occurs. Should the recycling of the casing be of interest to a recycling company, this solution would not qualify.

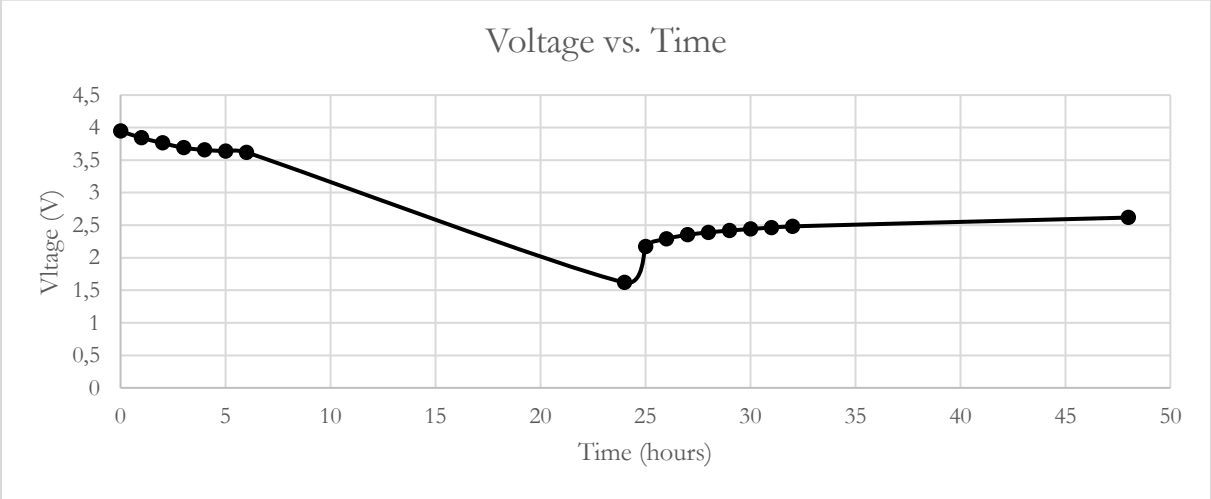

Figure 21: salt solution discharge using $NaNO_2$ solution

Figure 22: showing corrosion at welding points and blue-green crystal formed in $NaNO_2$ solution

4.2.6 Sodium Nitrate, $NaNO_3$

Ions in solution before electrolysis:

$NaNO3\ (s) + H2O\ (l) \rightarrow Na^+\ (aq) + H^+\ (aq) + NO_3^-\ (aq) + OH^-\ (aq)$ (32)

During electrolysis

Possible reactions at the Anode:

$Na^+(aq) + e^- \rightleftharpoons Na(s)$ E0= -2.71V (33)

$2H^+\ (aq) + 2e^- \rightleftharpoons H_2(g)$ E0= 0.0V (34)*

Possible reactions at the Cathode:

$2H_2O\ (l) \rightleftharpoons O_2\ (g) + 4H^+\ (aq)$ E0= -1.23V (35)*

$NO_3^-\ (aq) + H_2O\ (l) + 2e^- \rightleftharpoons NO_2^-\ (aq) + 2OH^-\ (aq)$ E0= 0.01V (36)

$2\ NO_3^-\ (aq) + 2H_2O\ (l) + 2e^- \rightleftharpoons N_2O_4\ (g) + 4OH^-\ (aq)$ E0= –0.85V (37)*

The experiment was able to undergo 24 hours of discharging (see Figure 23). Post discharge, the casing appeared to have undergone complete uniformed corrosion with possible black nickel oxide forming on the positive electrode (see Figure 24). Behind the terminal, another type of corrosion can be observed. It is likely that over a longer submersion period, complete corrosion through the casing would occur.

The starting pH for this solution was 5.93 and the final pH was 11.35. The solution started as weakly acidic, likely due to the competition between NaOH and HNO_3 in solution. During electrolysis, the solution becomes increasingly basic, suggesting reaction 37 was taking place producing nitrogen tetroxide. There is little bubble production observed in this solution with bubbles forming at both terminals and remaining stationary, that is, not rising to the surface of the solution. Since the positive terminal becomes completely oxidized, oxygen is likely formed at the positive terminal as in reaction 35 and reacts with the casing. Hydrogen is also likely formed as in reaction 33.

As in the previous solutions, it can be seen that the rate of discharge is slow for the first six hours, meaning that there is a rapid increase in the rate of discharge during the un-tested hours. This solution approaches a limit at ~2V, far higher than the previous solutions in addition, voltage rebound in this solution is almost entirely inexistent. The battery remained at ~2V days after the discharge process was stopped. There are two possible reasons for this lack of rebound, one, is that the corrosion of the positive terminal introduces an artificial resistance, making the voltage appear lower than it is in reality. The second, is that there has been some penetration of the casing and leakage of the electrolyte or active material, causing the potential between the poles to appear lower since there is lesser material to conduct the electrons. In either case, this solution is not suggested for salt solution discharge on an industrial scale due to corrosion of the casing and possible leakage of the materials within the cell.

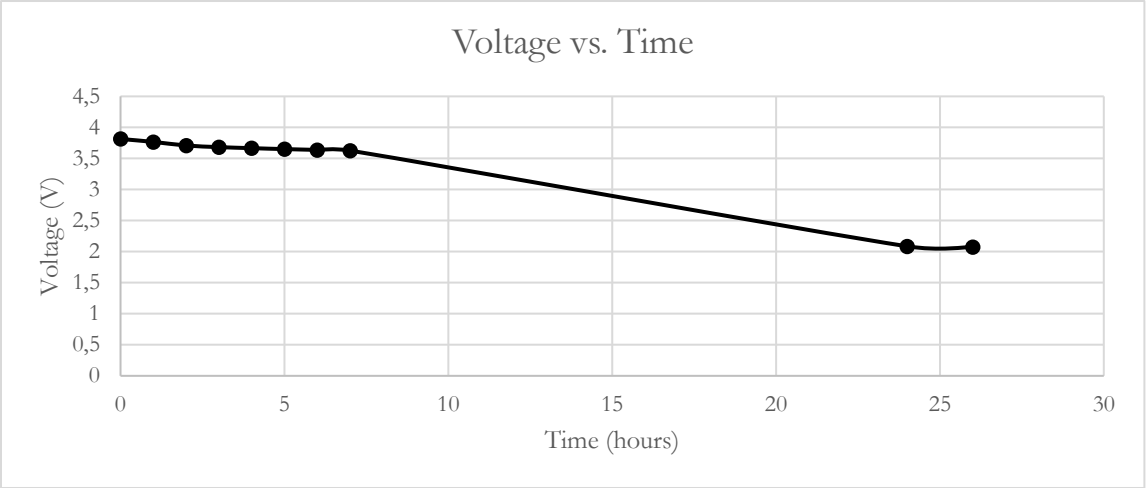

Figure 23: salt solution discharge using NaNO3

Figure 24: uniformed corrosion of positive terminal

4.2.7 Potassium Carbonate, K_2CO_3

Ions in solution before electrolysis:

K_2CO_3 (s) + $2H_2O$ (l) → $2K^+$ (aq) + $2H^+$ (aq) + CO_3^{2-} (aq) +$2OH^-$ (aq) (38)

During electrolysis

Possible reactions at the Anode:

$K^+(aq) + e^- \rightleftharpoons K(s)$ E0= -2.93V (39)

H_2O (l) + $2e^- \rightleftharpoons H_2$ (g) + $2OH^-$ (aq) E0= -0.83V (40)*

Possible reactions at the Cathode:

4 OH^- (aq) ⇌ O_2 (g)+ $2H_2O$ (l) + $4e^-$ E0= -0.40 (41)*

$2CO_3^{2-}$ (aq) ⇌ $2CO_2$ (g) +O_2 (g)+$2e^-$ E0= -1.90 to -1.95 (42)*

The experiment was able to undergo 24 hours of discharging without visible corrosion (see Figure 25). Post discharge, the casing appeared completely intact. The limit of water splitting is observed in this solution at 1.683V. The voltage rebound in this solution is rapid, with the voltage arriving at 2.5V two hours after removal from solution. This cell was not cycled prior to submersion.

The solution had a pH of 11.51 at the beginning of the experiment and 11.42 at the end, suggesting a weak base or dilute strong base was in solution. The base was likely potassium hydroxide (KOH). Bubble

production was observed in this solution until ~2V therefore, it is likely that carbon dioxide, oxygen and hydrogen gases were formed according to reactions 40, 41 and 42. Since the solution became slightly less basic, it is possible that reaction 42 is the main reaction with secondary amounts of reaction 41 forming water and consuming the base in solution. After ~2V, reaction 40 and 41 take over, the net reaction being water splitting. Since this discharge halts at around 1.683V it is likely that the limit of water splitting is slightly lowered when compared with Na_2CO_3 due to ease of ionization. This solution is strongly recommended for salt solution discharge at an industrial scale.

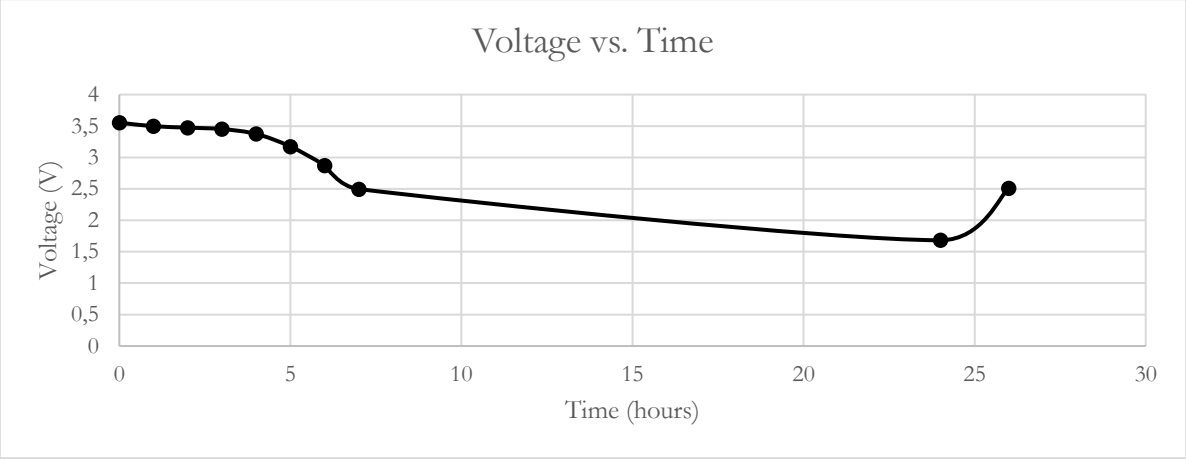

Figure 25: salt solution discharge using K_2CO_3 solution

4.2.8 Comparison of all 7 solutions

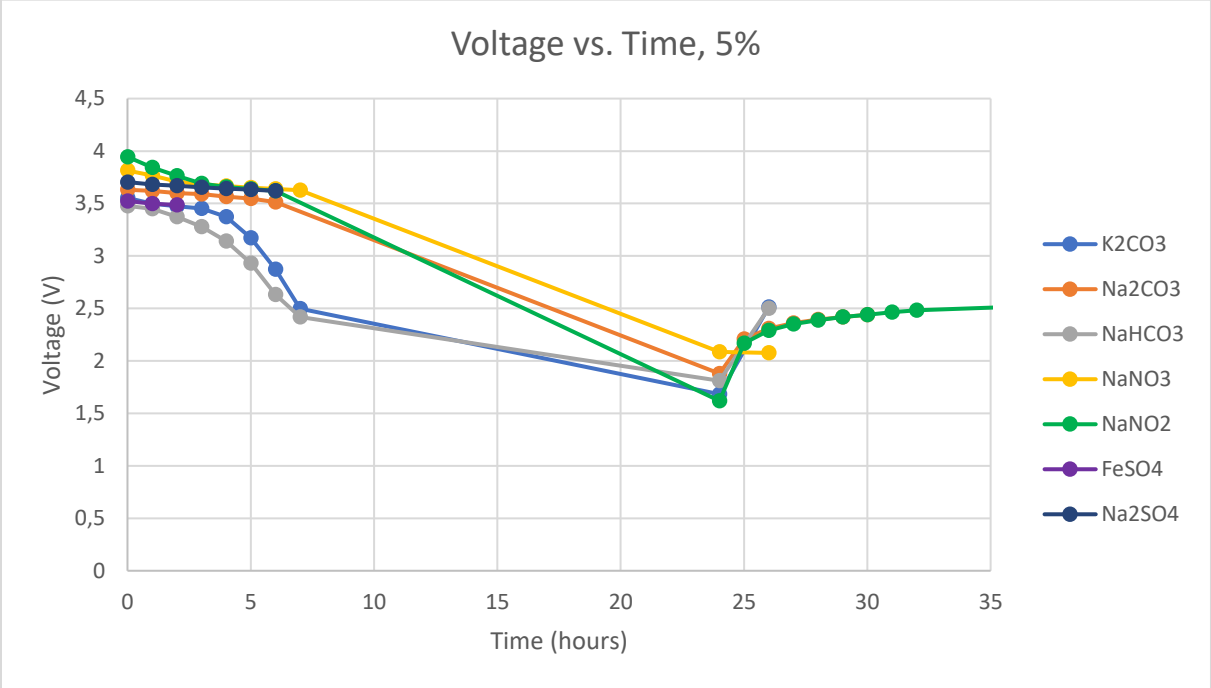

Figure 26: showing comparison of all 7 salt solutions tested at 5 wt%

Na_2CO_3 and $NaNO_2$ rebound far more slowly than $NaHCO_3$ and K_2CO_3 (see Figure 26). The cells used in the former two experiments were cycled prior to submersion, meaning they were purposefully 'aged'. It is unclear why the latter two display more rapid rebound rates although they were not purposefully 'aged'. The observation made here is not in line with that of Qian et al. however, it is possible that there are secondary effects in solution where $NaHCO_3$ and K_2CO_3 penetrate the cell in ways not visible to the eye. Further tests would be required to understand the mechanisms is occurring in solution (Qian, et al., 2019).

$NaNO_2$ and K_2CO_3 arrive at the lowest voltages in solution due, likely, to competing reactions and ease of ionization respectively. The carbonates have the highest rate of discharge with bicarbonate being the most rapid. However, it is worth noting that the cells in the K_2CO_3 and $NaHCO_3$ solutions started at a lower voltage than the others. The other solutions (Na_2CO_3, $NaNO_3$, $NaNO_2$) started at or above the nominal (operating) voltage, thus had a linear discharge for a period of time as the capacity of the cell was depleted. After the capacity of the cell was depleted, the other solutions likely had a discharge rate similar to that of K_2CO_3 and $NaHCO_3$. With that in mind, $NaNO_2$ had the fastest rate of discharge since it started at the highest voltage and discharged to the lowest. However, $NaNO_2$ displays corrosion. Should a recycling company be unconcerned about the state of the casing, or at least the positive terminal, then $NaNO_2$ would be the strongest candidate. However, should the casing be of interest, one of the carbonates is suggested.

It is difficult to assert whether or not conductivity plays a major role in the rate of discharge since a direct comparison of the salt solutions is not possible from these tests. Nevertheless, due to the low conductivity of $NaHCO_3$, the solution would be able to accept a battery pack of over 700V before arcing, making it a strong candidate for industrial use (see Table 2). $NaHCO_3$ also displays no corrosion further strengthening its position. K_2CO_3 and $NaNO_2$ would be poor candidates since both have higher conductivities than NaCl at 3.5 wt%.

In order to better understand the solutions and their rates of electrolysis, in the coming section, concentration and temperature are varied to determine if specific conditions lower the corrosion potential of some of the salts and to obtain a better direct comparison of the discharge/electrolysis rates. It is worth noting that submerging battery packs in solutions with a higher conductivity than 50mS/cm (the conductivity of sea water at 3.5 wt%) is not suggested. The following tests are meant solely to have a clearer understanding of the discharge and electrolysis mechanisms.

Table 2 showing factors affecting electrolysis

Solution	**Ionic Strength**	**Conductivity (mS/cm)**	**Theoretical Starting Current* (A)**	**Maximum Voltage before arcing (V)**
Na_2SO_4	1.05	42.7	0.13	527
$FeSO_4$	1.32	-	-	-
$NaHCO_3$	0.6	31.4	0.1	717
Na_2CO_3	1.5	47.0	0.15	479
$NaNO_2$	0.72	57.1	0.18	394**
$NaNO_3$	0.6	46.2	0.14	487
K_2CO_3	1.1	58.0	0.18	387**

*calculated

** conductivity higher than NaCl at 3.5 wt%, true maximum voltage is likely much lower

4.3 Salt Solution Discharge Under Various Conditions

The solutions that were able to undergo 24 hours of discharge at 5 wt% without complete corrosion of the casing ($NaHCO_3$, Na_2CO_3, $NaNO_2$, NaNO3 and K_2CO_3) were tested at 10 wt% and at 5 wt% with heat. At 10 wt%, the reactions were rapid enough to have a clearer understanding of what was happening in solution. Additionally, the starting voltage was held constant so that all conditions would remain the same. Of the solutions, potassium and sodium carbonate displayed no corrosion and an improved discharge rate. Therefore, the two underwent an additional test at 10 wt% with heat.

It was assumed that the electrolysis reactions would be the same but at an increased rate due to the introduction of more ions and/or heat. For information on the likely reactions please see section 4.2 above.

4.3.1 Sodium hydrogen carbonate, NaHCO3

4.3.1.1 10 weight%

There was no visible corrosion of the cell casing after 24 hours of discharge (see Figure 27). The discharge curve closely follows that of 5 wt% until 3V, after which the discharge rate is more rapid. Similar to at 5 wt%, the solution produces gas bubbles until ~2V, likely a mix of oxygen, hydrogen and carbon dioxide. The starting pH at 10 wt% was higher than 5 wt% (8.15 vs. 7.9 respectively) although the discharge ends at the same pH of 8.56, suggesting that the same mechanism is occurring in both solutions. However, voltage rebound at 10 wt% is much slower than that at 5 wt%, for known reasons.

4.3.1.2 5 weight% heated to 40-50°C

A black precipitate was deposited on the positive terminal of the cell after 24 hours (see Figure 28). The precipitate could easily be removed by a towel. It is likely some product of oxidation at the cathode though it is unclear what the composition of the precipitate is. Aside from the precipitate, the cell casing appeared intact. It is possible that some dissolution of the casing does occur and the dissolved metals are then oxidised at the positive terminal. This observation was also made by Shaw-Stewart but without the addition of heat (Shaw-Stewart, et al., 2019). Further research into the composition of the precipitate and the mechanism of its deposition would need to be understood in order for this solution to be used at an industrial scale in this condition. That being said, there is very little improvement in the rate of discharge for this solution at 10 wt% and 5 wt% with heat likely because the solution approaches saturation at just over 8 wt% (see Figure 27). The major improvement under these conditions is the rebound time, which is almost identical at 10 wt% and 5 wt% with heat. Kwade et al. proved that cells short-circuited when warm experience a slower rebound than when cool (Kwade & Diekmann, 2018). It is possible that the increased concentration has a similar effect on the cell, though it is unclear why.

This solution is most suitable at 5 wt% at room temperature for battery packs but could be used at 10 wt% for individual cells with a maximum voltage of 4.2V. The discharge time for this solution is greater than 4 hours.

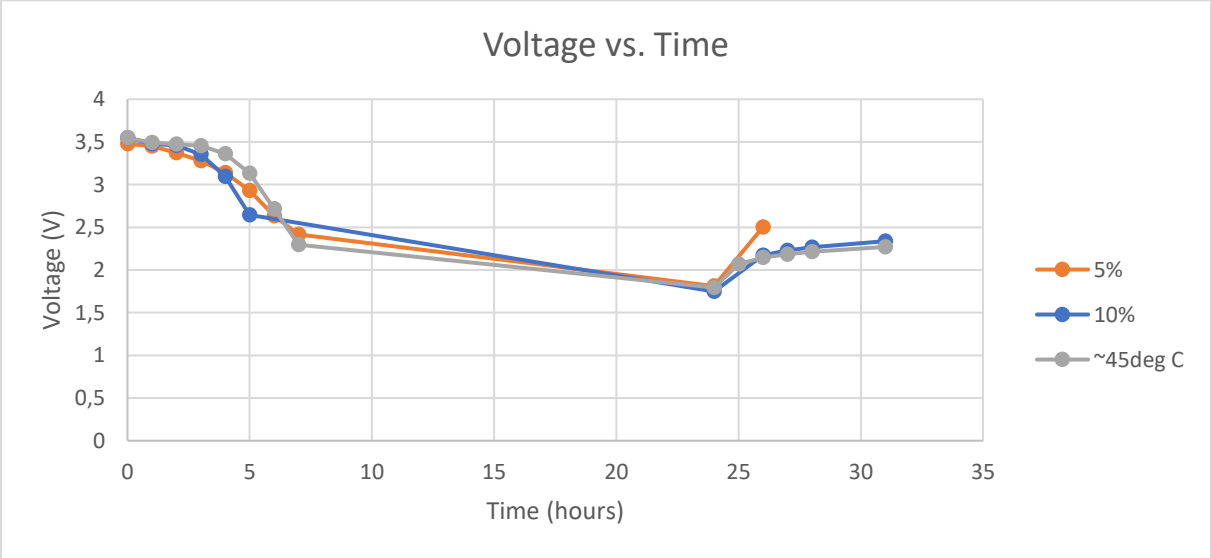

Figure 27: showing $NaHCO_3$ salt solution discharge at 10 wt% and 5 wt% heated conditions compared with 5wt% at room temperature

Figure 28: deposition onto the positive terminal in the ~45°C solution

4.3.2 Sodium Carbonate, Na_2CO_3

4.3.2.1 10 weight %

There was no visible corrosion of the cell casing after 24 hours of discharge (see Figure 29). The discharge rate at 10 wt% is significantly faster than that at 5 wt% although it is difficult to directly compare the two since they had different starting voltages. Similar to at 5wt%, the solution produces gas bubbles until ~2V, likely a mix of oxygen, hydrogen and carbon dioxide. The starting and ending pH at 10 wt% was higher than 5 wt% (11.57-11.42 vs. 11.14-10.97 respectively) however, it is likely that the same mechanism is occurring in both solutions. Voltage rebound at 10 wt% is slower than that at 5 wt% but follows a very similar trend, indicating that the increased current due to the increased ions in solution at 10 wt% has not 'aged' the cell as much as at 5 wt% (Qian, et al., 2019). It is unclear what the mechanism for this 'ageing' is. The lower limit in solution in 1.624V, lower than that at 5wt%.

4.3.2.2 5 weight % heated to 40-50°C

There was no visible corrosion of the cell casing after 24 hours of discharge (see Figure 29). The discharge rate at 5 wt% with heat is significantly faster than that at room temperature and slightly faster than at 10 wt%. Similar to at room temperature, the solution produces gas bubbles until ~2V, likely a mix of oxygen, hydrogen and carbon dioxide. The starting and ending pH of the heated solution was almost identical to that of the room temperature solution (11.13-11.00 vs. 11.14-10.97 respectively) suggesting that the same mechanism is occurring in both solutions. The voltage rebound of the heated solution is slower than at room temperature 5wt % and at 10 wt% though all three follow a similar trend. This observation is in line with that of Kwade et al. (Kwade & Diekmann, 2018). The lower limit in solution in 1.624V, lower than that at room temperature and at 10 wt%.

4.3.2.3 10 weight% with heated to 40-50°C

There was no visible corrosion of the cell casing after 24 hours of discharge (see Figure 29). The discharge rate at 10 wt% is the fastest of the solutions though it follows a similar trend to that at 5 wt% with heat. Similar to the other conditions, the solution produces gas bubbles until ~2V, likely a mix of oxygen, hydrogen and carbon dioxide. The starting and ending pH of the heated solution is similar to that of the room temperature solution (11.02-10.94 vs. 11.14-10.97 respectively) suggesting that the same mechanism is occurring in both solutions. The voltage rebound of the 10 wt% heated solution is the slowest of the four though it also follows a similar trend. However, the lower limit in solution in 1.624V almost identical to the heated solution at 5 wt%. 1.624V is likely the true water splitting limit in this solution.

It is strongly recommended that this solution be considered for salt solution discharge on an industrial scale. In order to fully optimise the process, it is recommended that the discharge be conducted at 10 wt% with heat for modules and cells but not for battery packs. Battery packs under 479V could be considered at 5 wt% or less at room temperature.

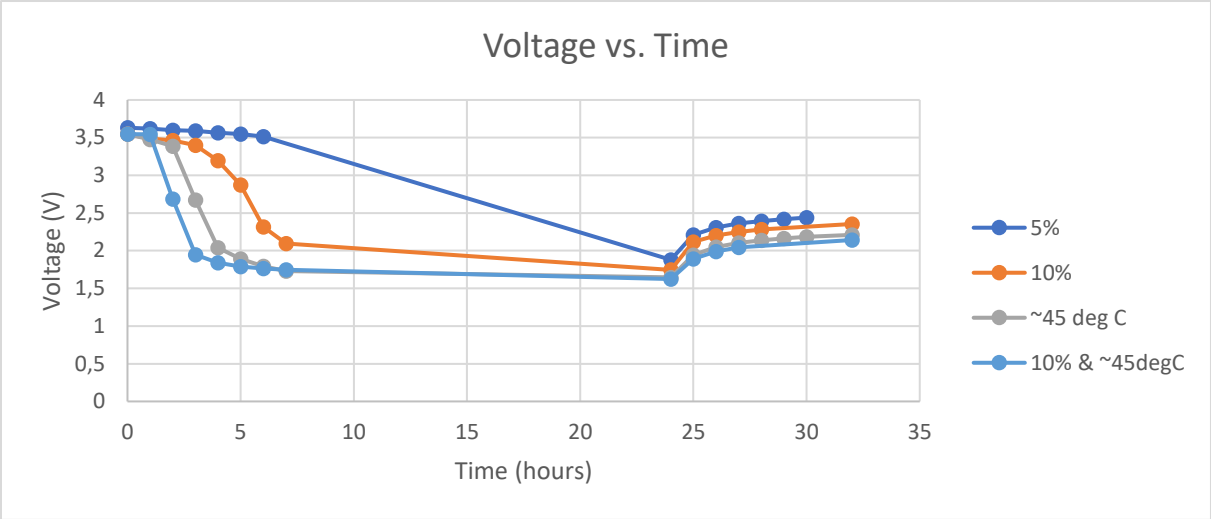

Figure 29: showing Na_2CO_3 salt solution discharge at 10 wt%, 5 wt% heated and 10 wt% heated conditions compared with 5wt% at room temperature

4.3.3 Sodium Nitrite, $NaNO_2$

4.3.3.1 10 weight %

There was no visible corrosion of the cell casing after 24 hours of discharge (see Figure 30). The discharge rate at 10 wt% is significantly faster than that at 5 wt% although it is difficult to directly compare the two since they have different starting voltages. Similar to at 5 wt%, the solution produces no gas bubbles. At 10 wt% the solution starts as a very weak acid (pH 6.2), as opposed to a weak base at 5 wt% (pH 8.15). However, they both arrive at similar final pHs at 11.22 and 11.65 respectively. It is likely that the same mechanism is occurring in both solutions. Voltage rebound at 10 wt% is slower than that at 5 wt% but follows a fairly similar trend, as would be expected. The lower limit in solution is 1.315V, lower than that at 5 wt% and almost at the theoretical limit of water splitting. It is likely that competing reactions predominate in this solution.

4.3.3.2 5 weight % heated to 40-50°C

There was no visible corrosion of the cell casing after 24 hours of discharge (see Figure 30). The discharge rate at 5 wt% with heat is significantly faster than at room temperature and slightly faster than at 10 wt%. Similar to at room temperature, the solution produces no gas bubbles. The starting pH of the heated solution was quite similar to that of the room temperature solution (8.46 to 8.15 respectively) however, the final pHs were quite different, suggesting some other reactions predominate (10.30 to 11.65 respectively). Furthermore, the lower limit in this solution is 1.128V, below the theoretical limit of water splitting, again suggesting that other reactions are controlling the reaction mechanism. The voltage rebound of the heated solution is very unusual and almost linear instead of logarithmic. It is likely that some penetration of the casing or other internal damage to the cell has occurred.

This solution would need to be analysed in depth before being recommended for salt solution discharge both for its corrosion potential and possible casing penetration.

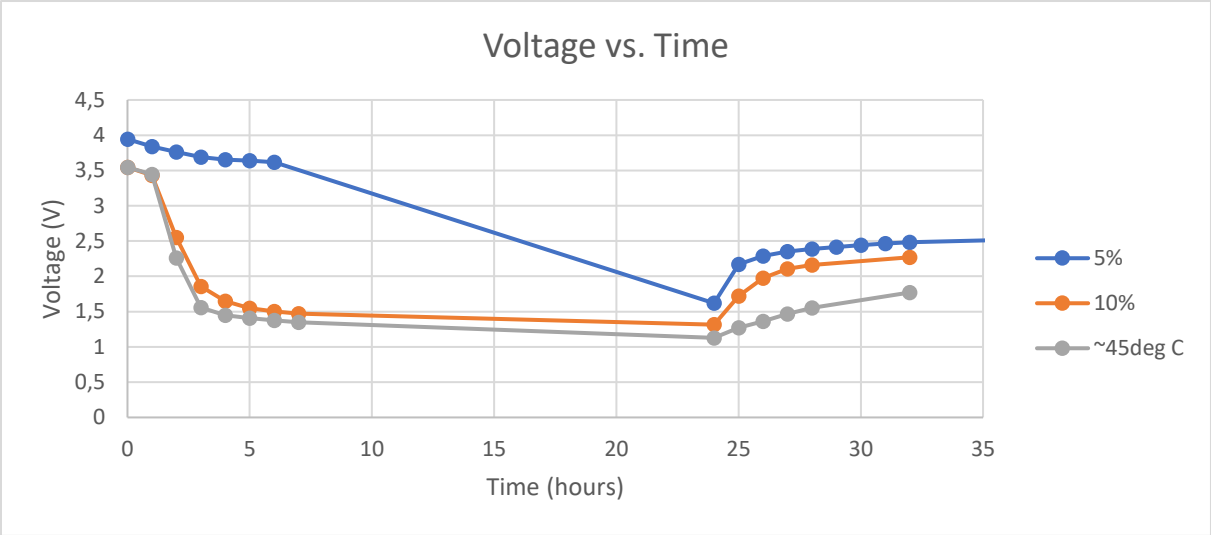

Figure 30: showing $NaNO_2$ salt solution discharge at 10 wt% and 5 wt% heated conditions compared with 5wt% at room temperature

4.3.4 Sodium Nitrate, $NaNO_3$

4.3.4.1 10 weight %

There was visible corrosion of the cell casing after 24 hours of discharge however, it was lesser than that at 5 wt% (see Figure 30). The discharge rate at 10 wt% is significantly faster than that at 5 wt% although it is difficult to directly compare the two since they have different starting voltages. Unlike at 5 wt%, the solution produces no gas bubbles. At 10 wt% and 5 wt% the solutions start as very weak acids (pH 6.7 and 5.93), then become basic by the end of the experiment (pH 10.34 and 11.35). Due to the differing end pHs and lack of gas production, it is possible that the mechanisms in solution are dissimilar and other half reactions predominate. Again, the lower limit in this solution is ~2V but in this case a somewhat normal voltage rebound is observed.

4.3.4.2 5 weight % heated to 40-50°C

In the heated solution, blue-green bacteria is formed on the battery and corrosion resembling the 10 wt% solution is seen (see Figure 31). The solution becomes yellow and translucent, it is unclear why this happens but may be due to the formation of the bacteria (see Figure 32). Due to the corrosion and bacteria formation, it is likely that the waste stream contains dissolved ions from the casing as well as other products of electrolysis. The starting pH of this solution is 7.52 and 8.97 at the end, which is very dissimilar to the 11.35 final pH observed in the room temperature solution. Additionally, bubbles are observed. The lower limit in this solution is 0.812V and voltage rebound is not observed, in fact, the voltage of the cell decreases with increasing time out of solution. It is highly likely that the cell was damaged in some way prior to the completion of the discharge, most likely around hour 4 or 5 where discharge rate appears to become linear instead of a decreasing exponent.

Due to corrosion, bacteria formation and the state of the solution, $NaNO_3$ is not recommended for salt solution discharge in an industrial scale under any condition.

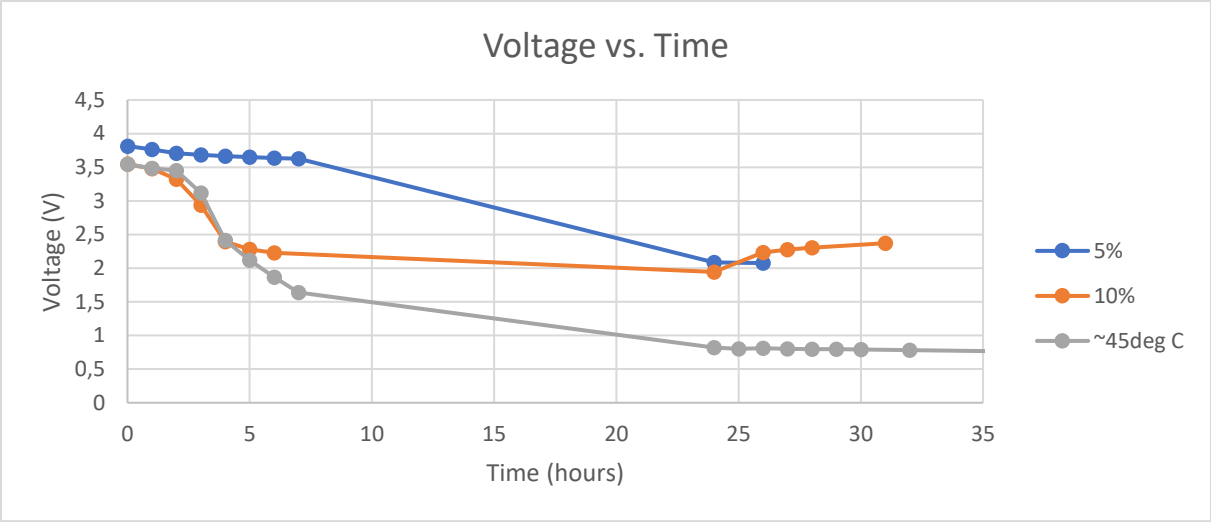

Figure 31: showing $NaNO_3$ salt solution discharge at 10 wt% and 5 wt% heated conditions compared with 5wt% at room temperature

Figure 32: showing (a) corrosion of the positive terminal after 24hrs of 10wt% discharge (b) blue-green bacteria forming on the cell in the heated solution (c) yellow translucent solution formed at the end of the heated experiment

4.3.5 Potassium Carbonate, K_2CO_3

4.3.5.1 10 weight %

There was no visible corrosion of the cell casing after 24 hours of discharge (see Figure 33). The discharge rate at 10 wt% is significantly faster than that at 5 wt%. Similar to at 5 wt%, the solution produces gas bubbles until ~2V, likely a mix of oxygen, hydrogen and carbon dioxide. The starting and ending pH at 10% was higher than 5% (11.92-11.71 vs. 11.51-11.42 respectively) however, it is likely that the same mechanism is occurring in both solutions. Voltage rebound at 10 wt% is at the same rate as at 5 wt%. It is unclear why the rebound at 10 wt% is not slower than at 5 wt% as has been observed in other solutions. Additionally, the voltage seems to peak then drop to a curve more like what would be expected. There could be a few reasons for this peak; it could be a real peak due to some unusual rebounding effect or it could be a fake peak taken as a misreading due to remaining electrolyte precipitating on the surface of the cell. A repeat of this test would be necessary to determine the true scenario. The lower limit in solution in 1.641V, identical to that at 5 wt% and similar to the 1.624V limit in Na_2CO_3 It is likely that this is the true lower limit for water splitting in carbonate solutions.

4.3.5.2 5 weight % heated to 40-50°C

There was no visible corrosion of the cell casing after 24 hours of discharge (see Figure 33). The discharge rate at 5wt% with heat is significantly faster than that at room temperature and slightly faster than at 10 wt%. Similar to at room temperature, the solution produces gas bubbles until ~2V, likely a mix of oxygen, hydrogen and carbon dioxide. The starting and ending pH of the heated solution is similar to that of the

room temperature solution (11.28-11.20 vs. 11.51-11.42 respectively) suggesting that the same mechanism is occurring in both solutions. The voltage rebound of the heated solution is slower than at 5 wt % and at room temperature 10 wt% but does not follow the expected trend. Instead, the rate of rebound decreases far less slowly than is normal. It is unclear why that happens. The lower limit in solution in 1.15V, lower than that at room temperature 5 wt% and at 10 wt% and lower than the theoretical limit of water splitting.

4.3.5.3 10 weight % heated to 40-50°C

There was no visible corrosion of the cell casing after 24 hours of discharge (see Figure 33). The discharge rate at 10 wt% is the fastest of the solutions though it is surpassed by the heated 5 wt% solution around hour 7. Similar to the others, the solution produces gas bubbles until ~2V, likely a mix of oxygen, hydrogen and carbon dioxide. The starting and ending pH of the heated solution is similar to that of the room temperature solution (11.21-11.12 vs. 11.51-11.42 respectively) suggesting that the same mechanism is occurring in solution. The voltage rebound of the 10 wt% heated solution is not initially the slowest of the four until the rebound of the heated 5 wt% solution passes it. The heated 10 wt% solution is the only of the four that follows a typical rebound trend. It is possible that at room temperature 10wt% and both the 5 wt% experiments, the casing of the cell is penetrated or corroded in some way that is not visible to the eye, causing unusual cell behaviour.

The lower limit in solution in 1.448V, suggesting the competing reactions occurring in the heated 5 wt% solution are also occurring in the heated 10 wt%, although to a lesser extent. Further tests would be necessary on this solution to determine what the competing reactions in the heated solutions are and to understand the unusual rebound behaviour. Shaw-Stewart observed that high pH solutions likely penetrated the casing of the cell in ways not visible to the eye, an observation in line with the unusual rebound curves observed (Shaw-Stewart, et al., 2019). It is not recommended that this solution be used for salt solution discharge on an industrial scale due to likely cell penetration.

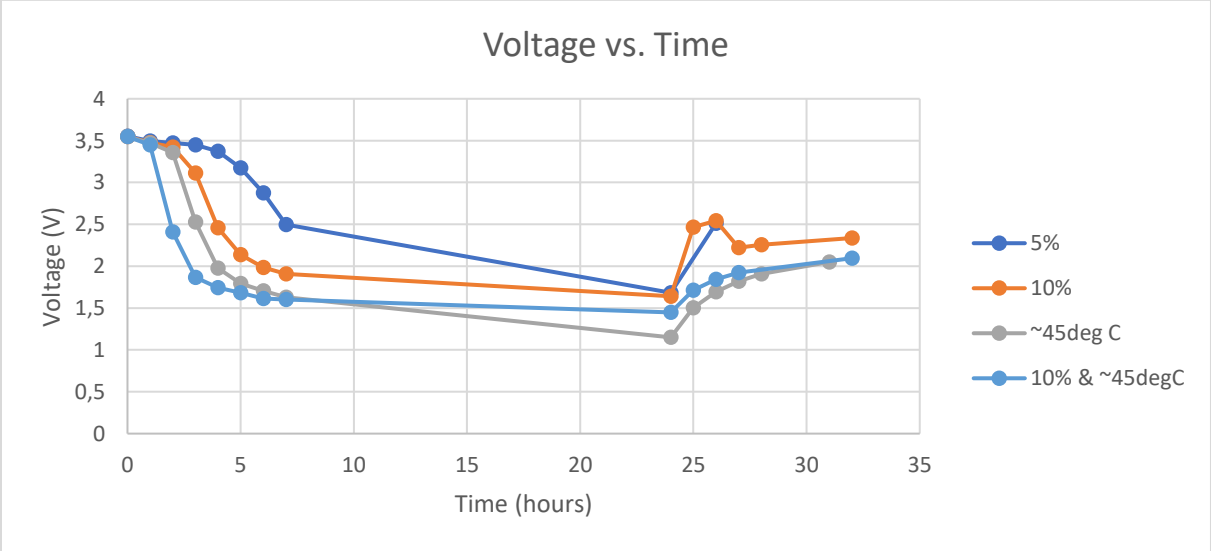

Figure 33: showing K_2CO_3 salt solution discharge at room temperature 10 wt% and 5 wt% heated and 10 wt% heated conditions compared with 5wt% at room temperature

4.3.6 All comparison at 10 weight%

$NaNO_2$ has the fastest discharge rate of all five solutions however, the rebound is unusually rapid (see Figure 34). This could be due to the low voltage achieved or to some internal damage to the cell. K_2CO_3 has the second fastest discharge rate but also has a rapid rebound for the first two hours, followed by a drop to a fairly normal rebound curve. It is unclear if the values recorded at hours 25 and 26 are 'real' or are due to precipitation of the electrolyte onto the cell. $NaNO_3$ has a similar discharge curve to K_2CO_3 but ends at a higher voltage. It is clear that some competing reactions forces $NaNO_3$ to terminate discharge at ~2V.

Na_2CO_3 and $NaHCO_3$ have the slowest discharge rates but follow similar curves and have fairly normal and similar rebound curves.

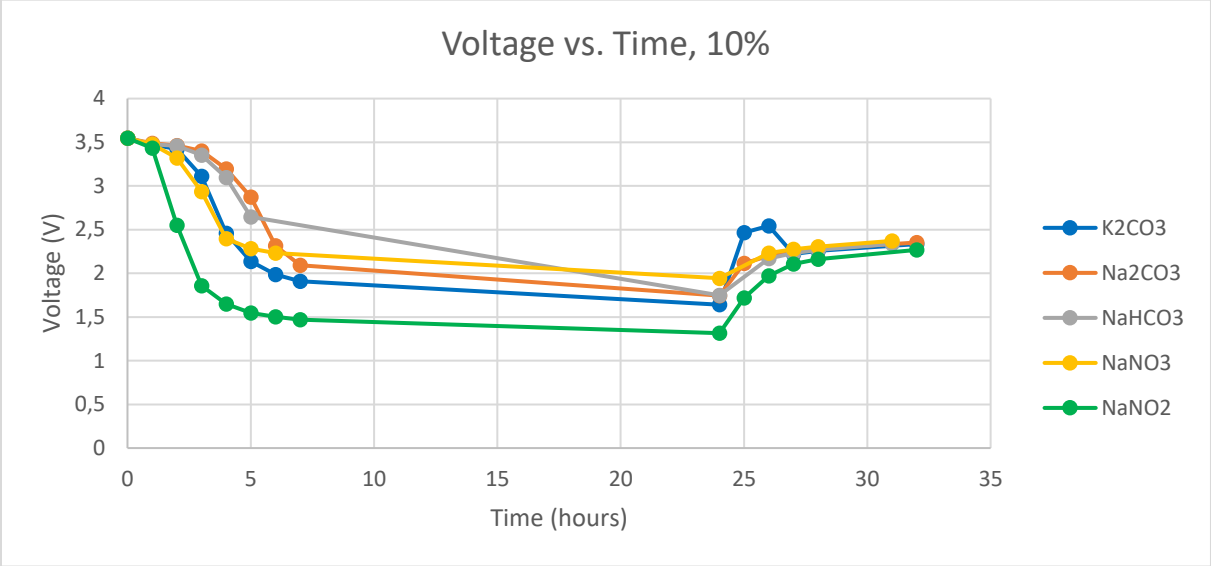

Figure 34: showing all 5 solutions at 10 weight%

Of the solutions at 10 wt %, only Na_2CO_3 and $NaHCO_3$ could be recommended for use at an industrial scale for cells and modules though it would not be recommended for battery packs since the conductivities are higher than NaCl 3.5 wt% (see Table 3).

It does not appear that conductivity is the only factor affecting the rate of electrolysis. Competing reactions, particularly in the case of $NaNO_2$ and $NaNO_3$, cause unusual discharge behaviour relative to the carbonates. Theoretically, K_2CO_3 should have the fastest discharge rate, but is far surpassed by $NaNO_2$ which has a lower conductivity and a lower ionic strength but a very high discharge rate. Na_2CO_3 has a high ionic strength which does not seem to contribute to a fast discharge rate. Far more analysis would need to be done to truly understand what the limiting and controlling factors are. It is possible that they differ by solution.

Table 3 showing factors affecting electrolysis at 10wt%

Solution	**Ionic Strength**	**Conductivity (mS/cm)**	**Theoretical Starting Current* (A)**	**Discharge Rate (in terms of place)**
$NaHCO_3$	1.2	73.8*	0.23	4th
Na_2CO_3	2.8	74.4	0.23	5th
$NaNO_2$	1.4	89.8*	0.28	1st
$NaNO_3$	1.2	82.6	0.26	3rd
K_2CO_3	2.1	109	0.34	2nd

*calculated

4.3.7 All comparison at 5 weight % heated to 40-50°C

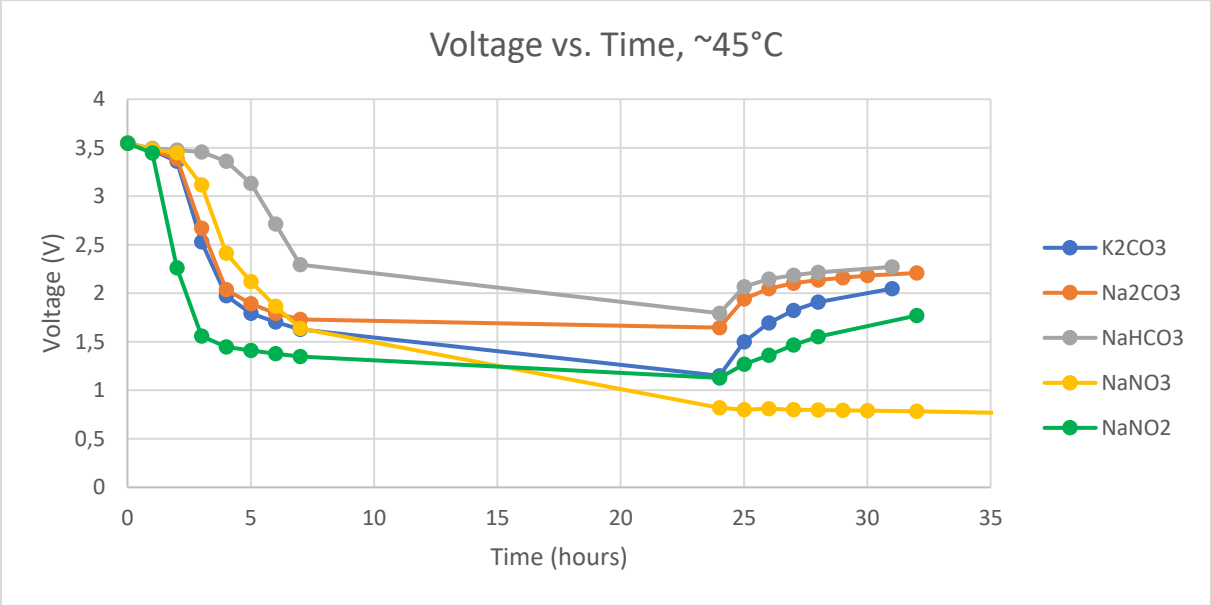

Figure 35 showing discharge curve for all 5 heated solutions at 5 weight%

Again, $NaNO_2$ has the fastest discharge rate of all five solutions however, the rebound is strangely linear instead of logarithmic (see Figure 35). It is likely that the cell was damaged in some way by this experiment. $NaNO_2$ already displayed corrosion at room temperature 5 wt%, so it is likely that the heated solution sped up this corrosion. However, the casing of the cell did not appear damaged.

Both $NaNO_2$ and K_2CO_3 surpass the limit of water splitting but have strange rebound curves. This may be due to damage of the cell or may simply be a product of such a deep discharge. $NaNO_3$ also surpasses the limit of water splitting but this is most likely due to damage of the cell since no rebound is observed at all. Again, K_2CO_3 has the second fastest discharge rate but an unusually rapid rebound. Na_2CO_3 discharges at a similar rate to K_2CO_3 but arrives at a higher final voltage and has a fairly normal rebound curve. $NaHCO_3$ has the slowest discharge and arrives at the highest final voltage but also has a fairly normal rebound curve.

Of the heated solutions at 5 weight %, only Na_2CO_3 and $NaHCO_3$ could be recommended for use at an industrial scale for cells, modules and with caution for battery packs since the theoretical conductivities should be increased by the addition of heat (see Table 2).

4.4 Metal Powder Discharge

As discussed in the background, few sources discuss or go into depth on how the metal powder discharge method works. It is likely that the powder forms part of a low resistance conductive path between the poles, allowing a high current to pass and causing a short circuit. It is also likely that the water acts as a thermal buffer, hindering thermal runaway. That being said, in literature, these tests were performed on 18650 cells probably at 2.1Ah (Gratz, Sa, Apelian, & Wang, 2014). It is likely that just water would be unable to deter thermal runaway in larger, higher capacity cells.

The LithoRec group cites discharging their batteries to a low electrical potential (1V) then short circuiting the batteries to lower the voltage rebound curve (Kwade & Diekmann, 2018). As a precaution, at full capacity (100% SOC), this method should only be conducted on cells with a maximum voltage of 4.2V due to arcing potential. Modules and battery packs can undergo this method only if they have already been discharged to a lower potential.

Th reason this method is of interest is that it lowers the discharge time for a cell to four hours, is able to discharge the battery to 0V and is able to short circuit the cell, thereby making it in line with the electronic load resistive discharge method (Gratz, Sa, Apelian, & Wang, 2014). It is also possible that the metallic

element will preferentially corrode over the cell, acting as a cathodic protector as discussed and tested by Ojanen et al. (Ojanen, Lundstrom, Santasalo-Aarnio, & Serna-Guerrero, 2018). When using a cathodic protector, Ojanen et al. observed that the discharge time was dropped to a few minutes. However, it is more likely that the metal provided a short circuit route with higher conductivity than the solution, thereby rapidly short circuiting it, rather than solely acting as a cathodic protector (see Figure 10).

With these details in mind, the metal powder discharge method was attempted. Aluminium foil and (steel) staples were used in place of steel chips as in the methodology described by Nan et al. and Gratz et al. Aluminium foil and staples were chosen as readily available, low cost options for proof of concept. The procedure for preparing the staples is described in the methodology section 3.5.

The aluminium foil test proved unsuccessful, so only the staples tests were continued. The limitation with using staples is that in order for the short circuit to occur, the staples must be perfectly oriented to be in contact with the positive and negative terminals. At the beginning of the experiment, when large amounts of energy is being expelled as heat in ohmic discharge, the short circuit is audible. After a few minutes, when the majority of the energy has presumably been expelled, there is no longer a sound and it is difficult to ascertain whether or not the discharge is occurring or if the cell has lost contact with the staples. The disconnection with the staples is visible in the data as voltage rebound. Future methods should use true steel chips or steel powder in order to combat this limitation.

4.4.1 Aluminum Foil with Distilled Water

No discharge was recorded after two hours of discharge with aluminum foil in water (Figure 36). It is unclear why there appears to be an increase in the voltage of the cells in the first hour however, by the second hour, the voltage of the cell is exactly the same as at the start of the experiment.

The positive terminal of the battery was deliberately placed in contact with the foil in the hopes of inducing discharge. Corrosion of both the positive terminal and aluminum foil is visible, suggesting that there may be momentary ion exchange when the battery comes in contact with the foil, but the discharge does not continue (see Figure 37). Due to the results of this experiment, the use of aluminum foil for metal powder discharge was discontinued.

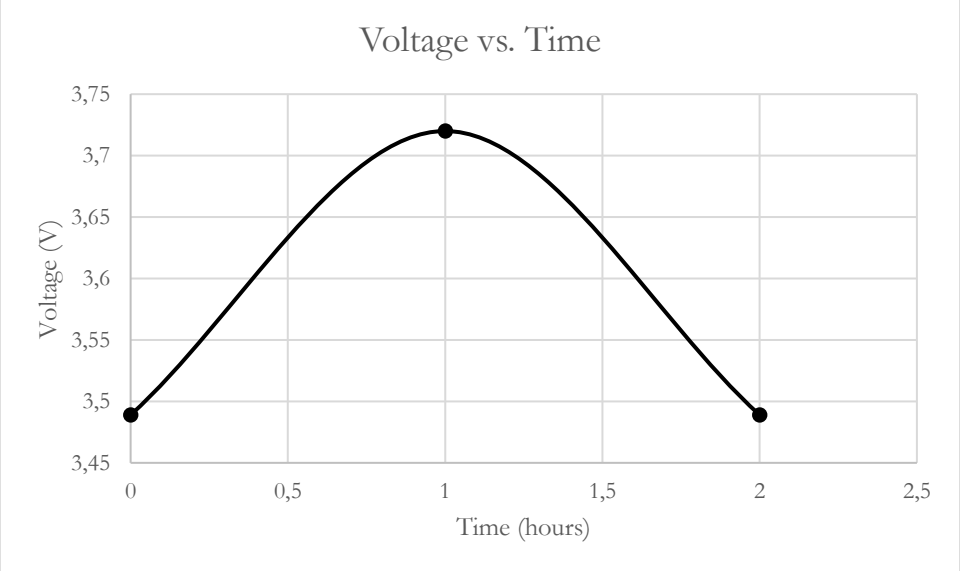

Figure 36: showing metal powder discharge using aluminum foil

Figure 37: showing corrosion of (a) aluminum foil and (b) positive terminal

4.4.2 Steel with Distilled Water

This test was attempted on two occasions. Once before the steel preparation method was decided upon then once after. In the first method some discharge was recorded (see Figure 38). Upon agitation of the beaker, at hour #2, glowing metal from short circuiting was seen. The staples and the casing demonstrated melting or corrosion (or both) at the contact point of the staples and the cell (see Figure 39). The effect appeared to be superficial and to be on both the positive and negative terminals. Further information would need to be gathered on the effect of the short circuiting on the casing and the steel and what effect that may have on the recyclability of the casing and the composition of the waste stream. The short-circuiting process lasted less than one minute and was audible. Further agitation to force a connection with the staples did not produce further short circuiting. It was concluded that the organic film that holds the staples together in packaging was hindering the electrical connection between the steel and the cell. It was from this revelation that the staple preparation method was borne.

In the second attempt, a full 24 hours of discharge elapsed (see Figure 40). The audible short-circuiting lasted several minutes. After one hour, the voltage of the cell was below 0.5V. Voltage rebound could be seen at hours 3 and 4 due to a disconnection between the staples and the cells. Nevertheless, the discharge appeared successful since after removal from solutions, the cell rebounded to ~0.5V and did not rise several weeks later. A far shorter discharge time could be envisioned for this method since the rebound voltage of the batteries is already less than 0.5V after one hour. An optimization would need to be done in order to determine the true time required.

The primary limitation of this method is the rusting of the steel chips (see Figure 41). Although the cell itself appears to be free from corrosion, the corrosion from the staples deposits on the casing. Additionally, for ease of re-use and sustainability, consistently destroying steel chips to discharge a cell is not practical. Therefore, other solutions were tested in the hopes of circumventing corrosion.

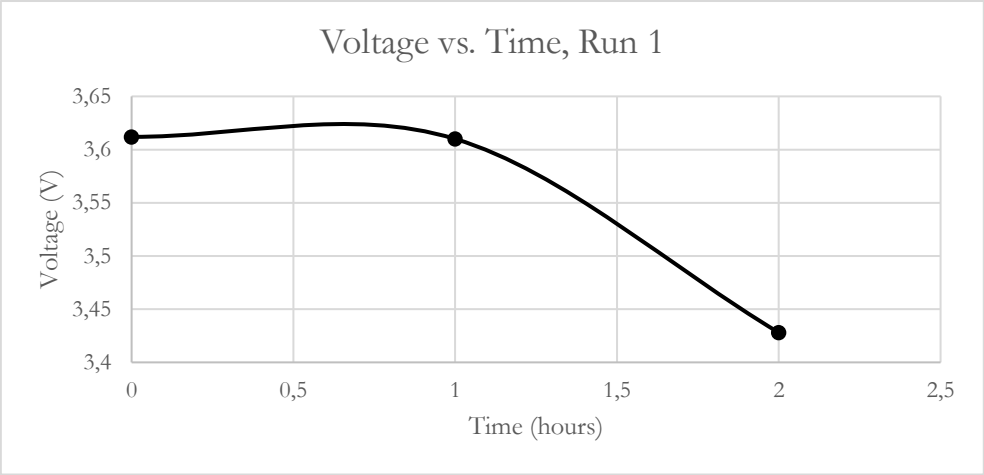

Figure 38: showing metal powder discharge using steel ships in the form of staples

Figure 39: showing melting of the casing and staples as a result of short circuiting

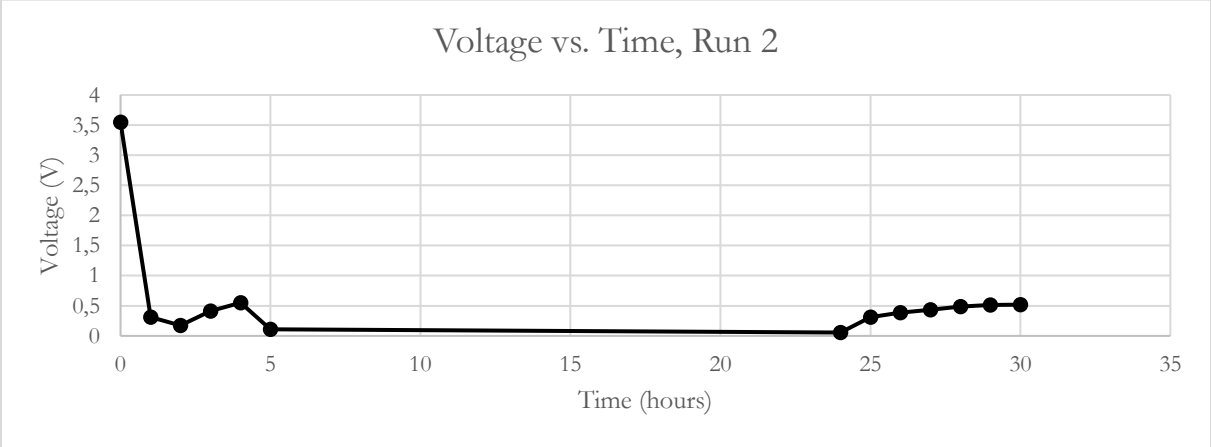

Figure 40: showing full 24-hour metal powder discharge

Figure 41: showing rusted staples after 24 hours in water

4.4.3 Sodium Hydrogen Carbonate, $NaHCO_3$

This method was also attempted in $NaHCO_3$ on two occasions. In both cases, short-circuiting stops after a total of 4 (Run 1) and 5 (Run 2) hours and does not continue, even upon agitation and forced connection with the staples. Thereafter, the cell voltage rebounds to around 1.7V in solution and continues to rebound to 2V out of solution. It is unclear why this occurs. Additionally, some rusting of the staples is visible although far less than in water. This solution is not recommended for metal powder discharge due to the corrosion of the staples and the inexplicable halted discharge after 4-5 hours.

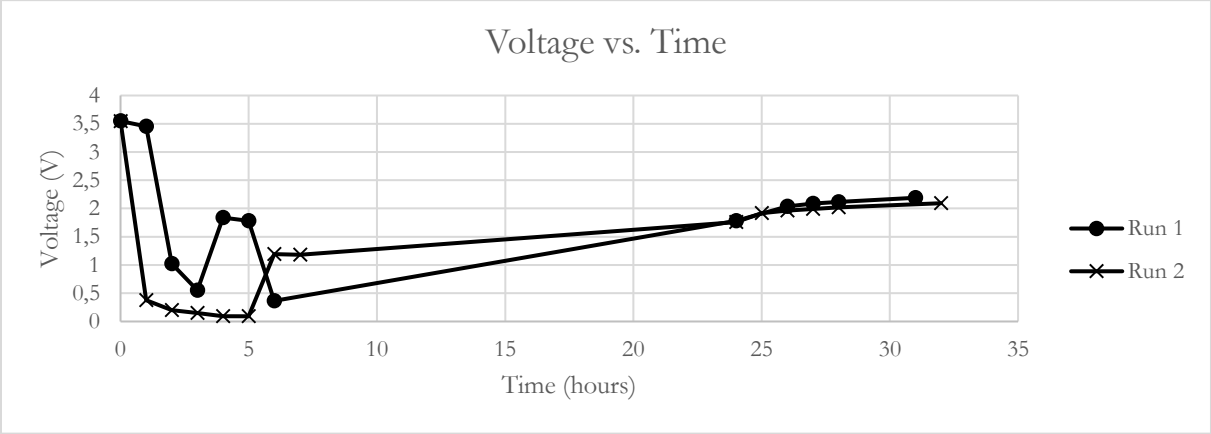

Figure 42: showing discharge curves for $NaHCO_3$ with steel

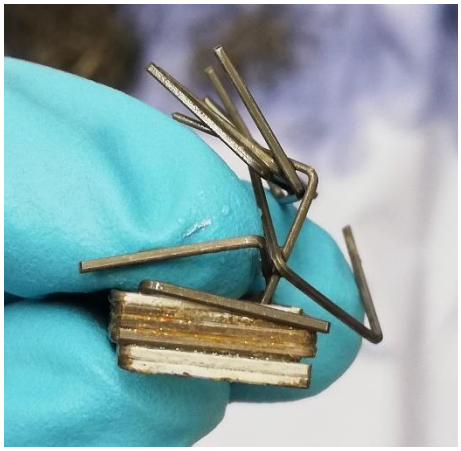

Figure 43: showing rusting of the staples post discharge in run 1

4.4.4 Sodium Carbonate, Na_2CO_3

After 3 and 5 hours, voltage rebound is visible due to improper connection with the staples. However, in the one hour of short circuiting between hours 3 and 5, the rebound rate is slowed by almost 0.04V. After the full 24 hours of short circuiting, the cell rebounds to ~0.7V in seven hours and remains at this voltage up to three days post discharge. The staples appeared to be completely intact post discharge and showed no visible signs of corrosion. Due to the state of the staples post discharge, it is possible that this solution could be used for metal powder discharge, however, some optimization for time would be required, that is, to lower the discharge time to 4 hours and keep the rebound to below ~0.5V.

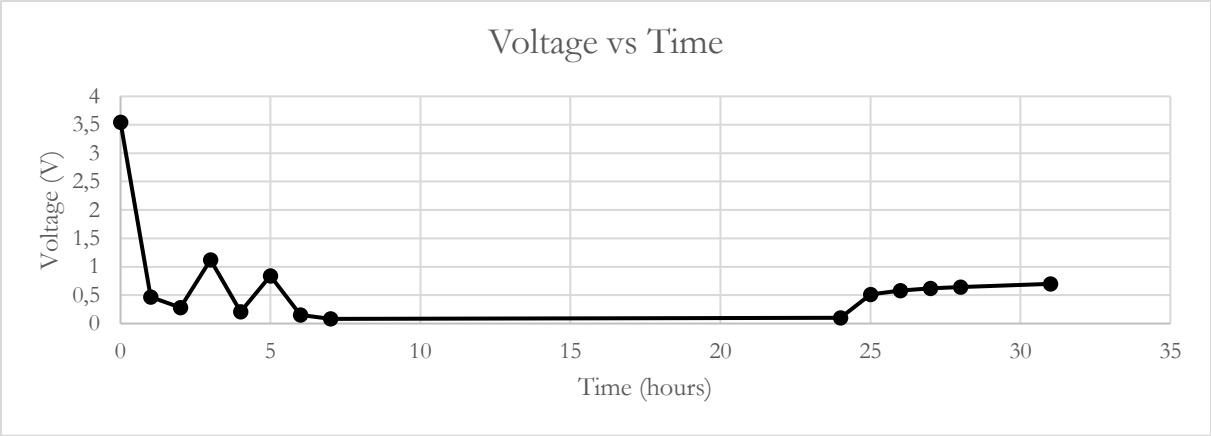

Figure 44: showing metal powder discharge in Na_2CO_3

4.4.5 Sodium Nitrite, $NaNO_2$

After 4, 5 and 7 hours, short-circuiting is halted due to the limitations of the experimental procedure/materials (see Figure 45). Since this solution was only attempted once, it is difficult to assert whether or not $NaNO_2$ has a limit to short circuiting in solution similar to $NaHCO_3$ or if the staples were disconnected from the cells during the overnight portion of the experiment. However, the total short-circuit time, like in $NaHCO_3$, is around 4 hours. A second run is suggested to determine if this observation is repeatable. The staples appear mostly intact after discharge though they appear not to retain the matte grey colour that the staples do in Na_2CO_3. There is also some amount of rust deposited on the positive terminal either from the staples or the oxidation of dissolved metals in solution (see Figure 46). Due to the disconnection with the staples, the cell voltage rebounds to almost 2V out of solution. Since the staples appear mostly intact post discharge, it is recommended that further tests be done on this solution to confirm the halted discharge and the corrosion products.

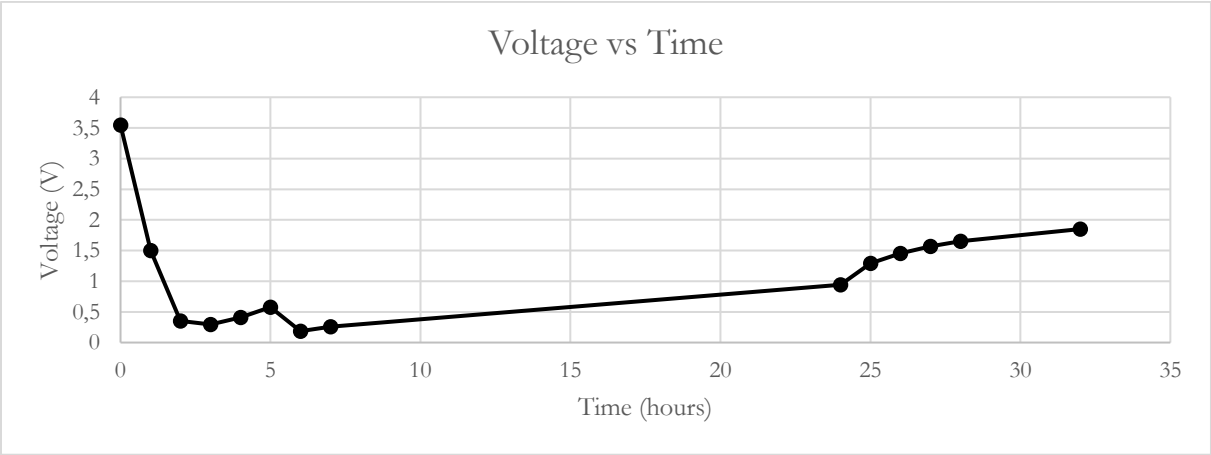

Figure 45: Metal powder discharge in $NaNO_2$

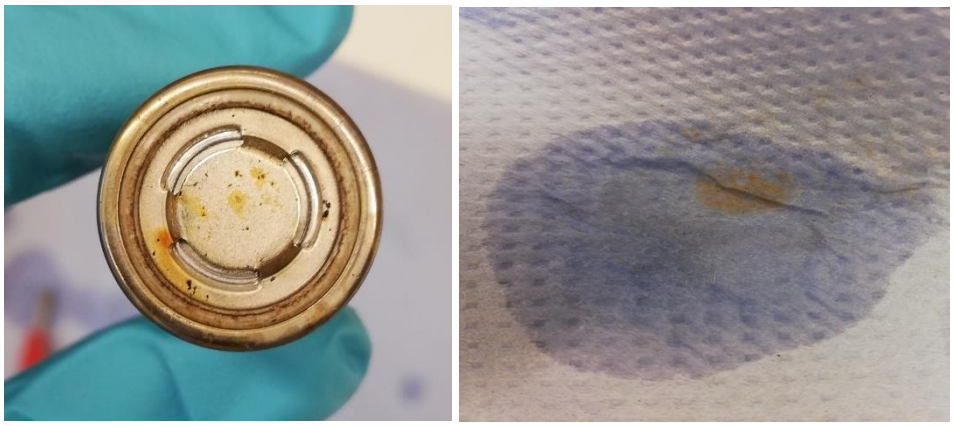

Figure 46: showing (a) deposition of rust(?) from the staples or from solution onto the positive terminal. Melted sections of the casing can also be seen where short circuiting occurred (b) the deposited rust(?) is easily removed by a towel.

4.4.6 Sodium Nitrate, $NaNO_3$

In this solution, the positive terminal becomes completely black, likely due to oxidation of the nickel and iron of the casing (see Figure 48). This type of corrosion is in line with the 5wt% at room temperature test. After one hour, small amounts of blue-green bacteria is seen on the battery, the bacteria becomes black after several hours of discharge. The staples also appear completely black post discharge, suggesting corrosion. The solution becomes yellow and translucent. It is likely that the change in colour of the solution is due to corrosion and the bacteria formation. The waste stream probably contains dissolved ions from the casing, the staples as well as bacteria and other products of electrolysis. Having undergone a total of 23 hours of short-circuiting, the voltage rebound in this solution is rapid, returning to over 1V eight hours post discharge. Rebound in this solution has consistently been unusual, suggesting possible damage of the internal materials of the cell. This solution is again disqualified for use at any scale.

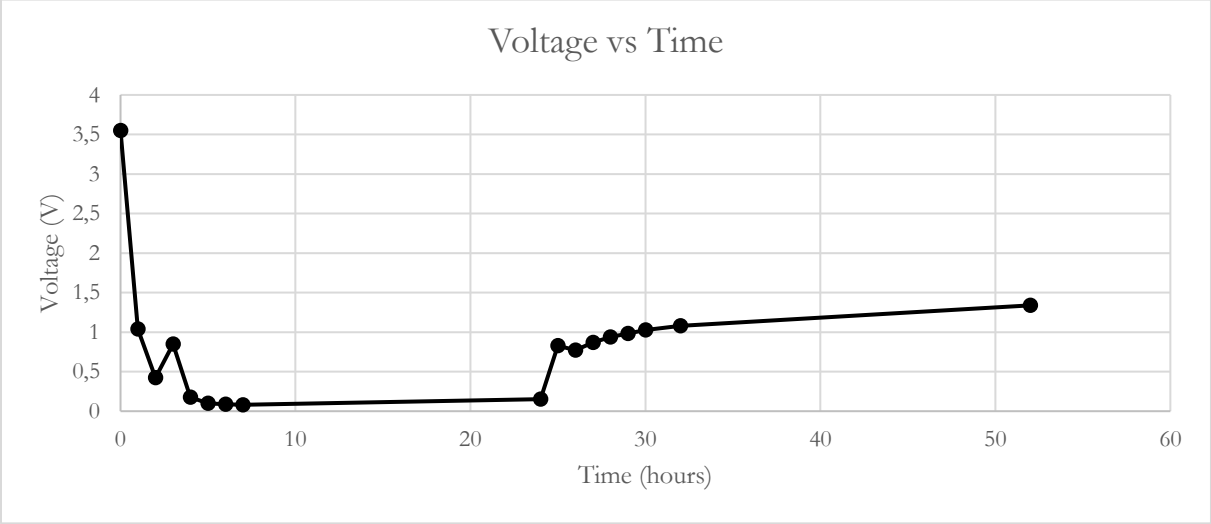

Figure 47: showing metal powder discharge in $NaNO_3$

Figure 48: showing (from top left) (a) corrosion of the casing and formation of blue-green bacteria after one hour (b) blackening of the positive terminal after 24 hours of discharge, (c) yellow-brown solution post discharge, (d) blackening of the staples post discharge

4.4.7 Potassium Carbonate, K_2CO_3

During hours 5 and 6, voltage rebound is visible due to improper connection with the staples. Both at hour 6 (in solution) and hour 25 (1 hour after the battery has been removed from solution) the voltage rebounds to 0.5V. It is possible that the cell could be short circuited for 5 hours, and the rebound would be somewhat faster but similar in shape to that after 24. If so, the discharge and short circuit time could be significantly shortened. The staples appeared to be completely intact post discharge and showed no visible signs of corrosion. Voltage rebound was to ~0.6V after 8 hours post discharge. Due to the state of the staples, it is possible that this solution could be used for metal powder discharge, however, some optimization for time would be required, that is, to lower the discharge time to 4 hours and keep the rebound to below ~0.5V.

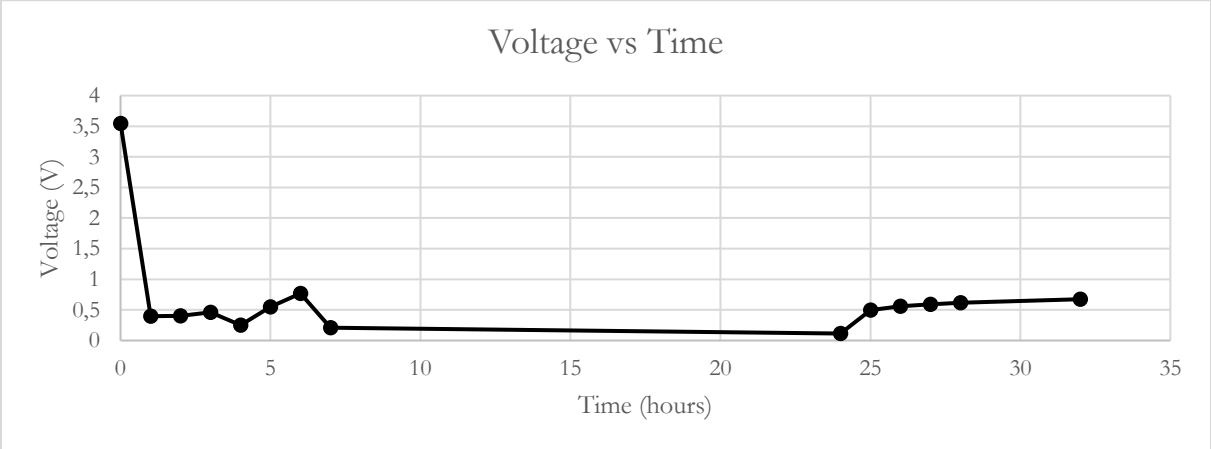

Figure 49: showing metal powder discharge in K_2CO_3

4.4.8 All comparison using metal powder discharge method with steel

From the solutions tested, distilled water with steel is the best solution to use to maintain the voltage of the cell at ~0.5V post discharge (see Figure 50). However, there is significant corrosion of the staples after 24 hours. Na_2CO_3 and K_2CO_3 closely follow water in the rate of discharge and rebound to approximately 0.6-0.7 V after several hours out of solution. Either of the two solutions could reasonably be used in this method. Though caution would have to be taken with K_2CO_3 due to possible cell penetration.

This method is ideal for cells so long as enough solution is provided to cool the cells and combat thermal runaway. For modules and battery packs, it is recommended that they are first discharged to a lower potential, then placed in solution to undergo short-circuiting via metal powder discharge.

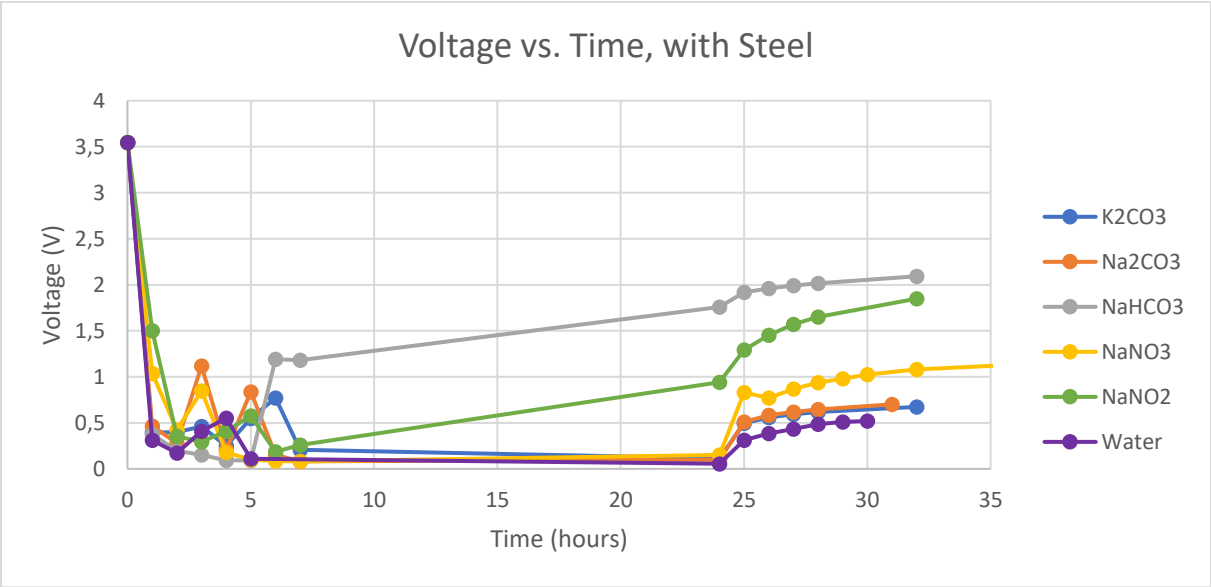

Figure 50: showing all comparison

4.4.9 Time Optimization

In order to determine if it is possible to lower the discharge time for the metal powder discharge method, a time optimization using 5 wt% Na_2CO_3 in a water bath at 50°C was prepared. The method was repeated for 6, 5, 4 and 3 hours to determine the shortest amount of time that could be undertaken to arrive at 0V and combat voltage rebound to greater than ~0.5V (see Figure 51). From the experiments, 4 hours appears to be the optimum, minimum, time for discharging.

5 wt% Na_2CO_3 in a water bath at 50°C for four hours is an ideal methodology for discharging cells for recycling. It could be conceived that this method is used with battery packs and modules that are already discharged to a low voltage (SOC 0%). However, the modules and battery packs should be under 500V at SOC 0%. At greater than 500V, there is a risk of arcing and resultant fire.

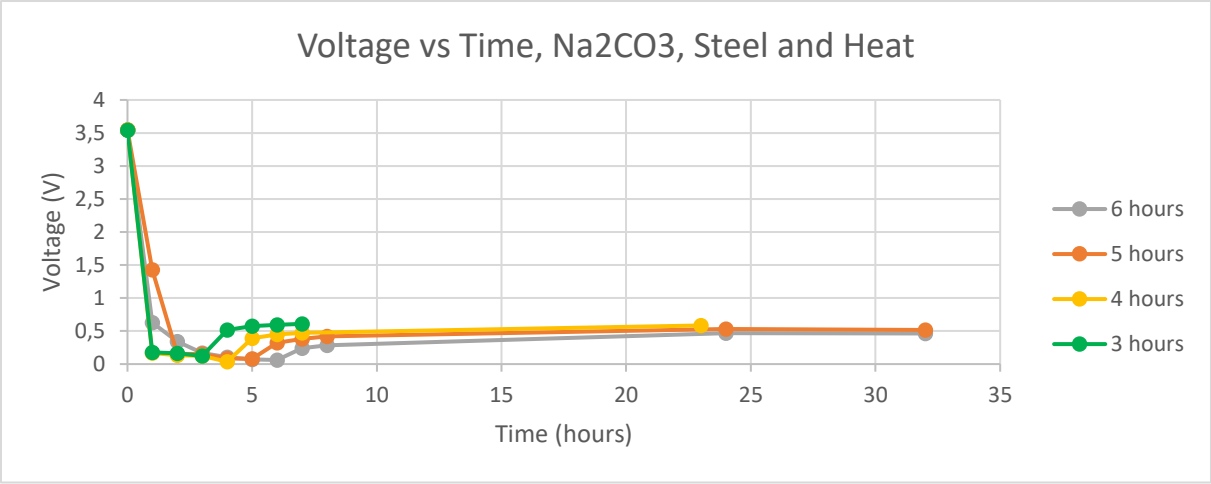

Figure 51: showing time optimization using 5wt% Na_2CO_3 in a water bath at 50°C

4.5 Proposed Procedure

The following procedure is proposed for recycling EV batteries. Though no EV batteries were tested in this thesis, the assumptions made leading to these conclusions are discussed in the previous sections.

4.5.1 Electronic Load

An electronic load with energy recovery can cost over 10'000 € (source withheld). Assuming each battery is delivered to the recycling facility at 30% SOC (the limit for air transportation), and assuming the average battery is 20kWh, then 5.7kWh is recovered from each battery (Elwert, et al., 2015). In a simplified, preliminary cost calculation, assuming an electricity cost of 0.19€/kWh in Sweden, just under 10'000 batteries would be required to recover the capital cost (Statista, 2018). A facility taking in 500 batteries a week would break even in less than six months (see Figure 52). Energy recovery makes resistive discharge an attractive option since there are cost and energy savings involved. Therefore, for high energy battery packs, resistive discharge is still the most feasible option particularly since directly short circuiting or submerging a high energy battery is not recommended. It is worth noting that in order to connect a battery pack to an electric load, regenerative or otherwise, the connection to the load must be made 'behind' the BMS to avoid the BMS controls (Hansson, 2019). With that in mind, each battery pack would need to have the top removed prior to discharging. Automation of the electronic load resistive discharge process is underway and would need to be perfected for industry (Kwade & Diekmann, 2018).

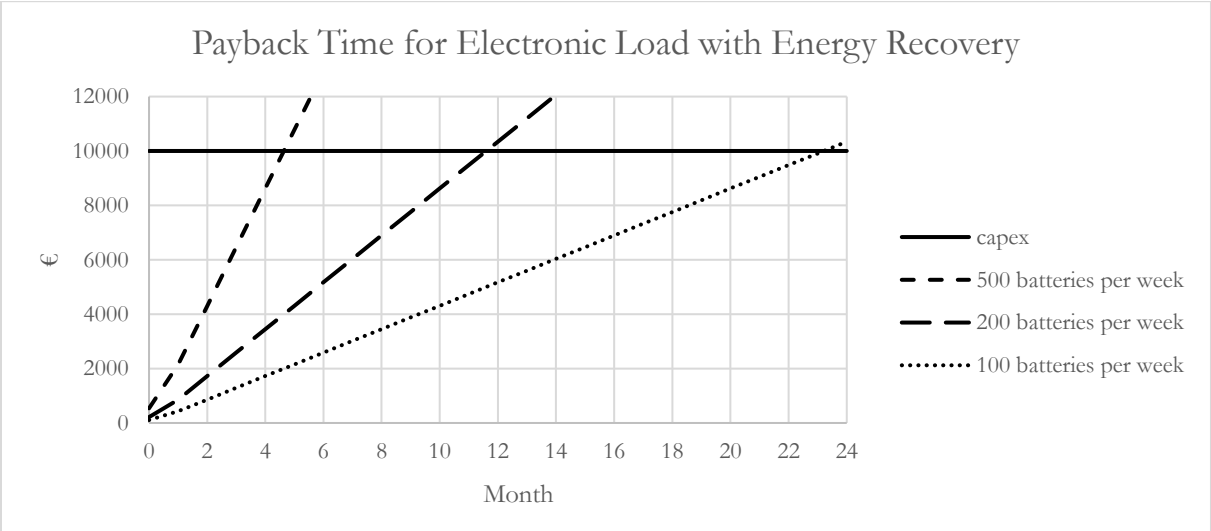

Figure 52: showing payback time for electronic load with energy recovery

The residual energy in a battery at 0% SOC is 1% of the capacity or 200Wh using the assumptions made above (Sonoc, Jeswiet, & Soo, 2015). Therefore, it is not feasible to use an electric load to discharge a battery pack delivered at 0% SOC. Instead, salt solution/metal powder discharge is suggested.

4.5.2 Combined Salt Solution/Metal Powder

The five salts which were tested under various conditions cost from 12 to 25 €/t, with the exception of K_2CO_3, which costs 1000€/t (see Table 4). The costs of each solution was considered when deciding upon the chosen method. Na_2CO_3 is the most consistent salt with fairly normal rebound curves under all conditions and no visible corrosion. Na_2CO_3 is also amongst the cheapest of the solutions. For this reason, it is suggested that Na_2CO_3 be used for salt solution discharge on an industrial scale.

For individual cells at any SOC, 50°C, 5wt% Na_2CO_3 with steel solution should provide no corrosion or arcing potential. Therefore, to maintain the discharging process at 4 hours, heated solutions are suggested. A comparison between the time saved and the energy required to heat the solution to 50°C should be conducted.

For modules and battery packs below 500V at 0% SOC, a two-step process is suggested. First the batteries should be placed in room temperature 5 wt% Na_2CO_3 to allow a deep discharge. Thereafter, the modules and battery packs could be placed in 50°C, 5wt% Na_2CO_3 with steel for four hours of short circuiting. Naturally, the two-step process would be longer than 4 hours. A time optimization would need to be conducted to determine if this process could be faster and the relevant energetic requirements.

It is of note that Na_2CO_3 produces carbon dioxide during electrolysis, which is contrary to IPCC goals. In order to mitigate this, the CO_2 could be captured and used in the inert atmosphere for crushing or other processes. The gases produced at the positive terminal increase the arcing potential of this solution. Therefore, a step-wise increase from cells to battery packs is suggested to check for the real-life voltage limit for arcing. The limit discussed in this thesis is theoretical.

Additionally, the steel required for short-circuiting was not considered since the crushed casing of the cells could be used in this application. It is conceivable that the solution post discharge contains trace amounts of dissolved casing and steel ions. Further tests would be required for confirmation but it is likely that the water can be treated by precipitation of the metals, including excess sodium, that would remain in solution.

Table 4: showing costs and other information for the salt solutions tested under various conditions. The costs are an average based on the Alibaba prices as of March, 2019 (Alibaba, 2019).

Salt	**Na_2CO_3**	**K_2CO_3**	**$NaHCO_3$**	**$NaNO_2$**	**$NaNO_3$**
Cost (€/tonne)	12.5	1000	12	24	20
State of Casing	Intact	Intact	Occasional Corrosion	Corrosion	Corrosion
Gases produced	CO_2, O_2, H_2	CO_2, O_2, H_2	CO_2, O_2, H_2	none	N_2O_4, H_2
Waste Stream	Colourless Solution	Colourless Solution	Occasional Precipitate	Precipitate	Precipitate
State of Staples	Intact	Intact	Slightly rusted	Slightly Altered	Blackened

4.5.3 Procedure by Item

Although not extensively discussed in this document, it has been suggested that critically damaged batteries, where the terminals within the modules or cells have been disconnected, cannot be discharged. In this case they will require special procedures. This is an area for significant development.

It is also worth noting that although the focus of this study is EV batteries, the recycling processes stated could be extrapolated to other types of Lithium-ion batteries for example other e-mobility applications, portables, industrial use, grid stability, home storage and renewables.

Based on the tests conducted in this thesis, and discussed in the previous section the following decision matrix is proposed for cells, modules and battery packs (see Figure 53):

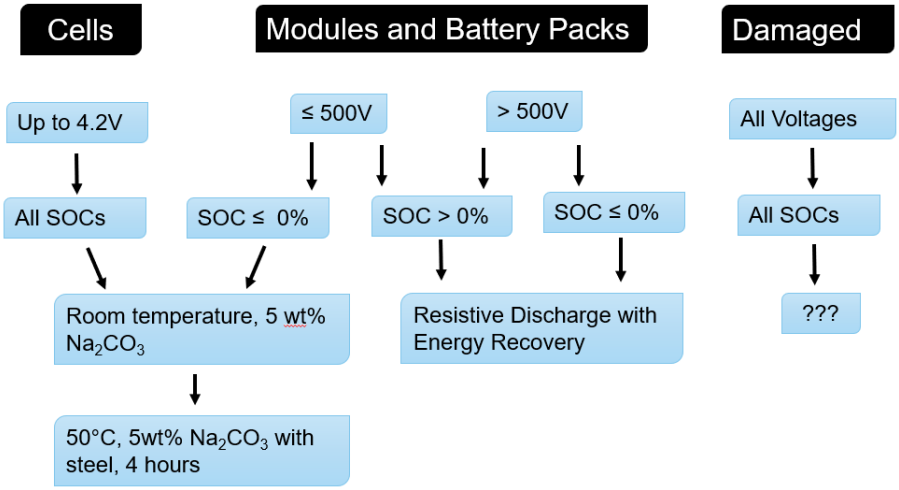

Figure 53: showing proposed discharge decision matrix

4.6 The future of recycling

Inductive discharging was briefly discussed in the background. It can be conceived that future EV batteries would be equipped with a pad for wireless charging since there is an increasing demand for wireless technology (WiTricity, n.d.). Therefore, the pads should be bidirectional so that all batteries entering the recycling facility can be discharged wirelessly. Since no physical connections to the batteries would be made, human contact with the battery would be nil.

Additionally, the BMS could also be accessed wirelessly or by infrared. It should be equipped with an 'override' feature for recycling so that when the BMS is activated during discharging, it receives a signal indicating that it should allow for a discharge to 0V but still provide information on the SOH of the battery in terms of voltage, current and temperature. Honda and WiTricity have already proven that the discharged energy can be recovered in a vehicle to grid operation so, energy recovery would also be built into this model (Tachikawa, Kesler, & Atasoy, 2018).

4.7 Sustainability

In order to limit global warming to 1.5°C as directed by the IPCC, the decarbonization techniques chosen must clearly mitigate global warming. An evaluation of the method(s) suggested in this thesis was not undertaken since it is still at the laboratory scale. Instead, evaluations of similar processes were reviewed in order to better understand the environmental implications of recycling.

The reviewed life cycle analyses (LCAs) evaluated recycling lithium-ion batteries under some or all of the following conditions (Gaines, Sullivan, & Burnham, Life-Cycle Analysis for Lithium-Ion Battery Production and Recycling, 2011) (Olofsson & Romare, 2013) (Buchert & Sutter, 2016):

- Cumulative energy demand in terms of MJ or BTU/t.
- Greenhouse gas emissions as global warming potential (GWP) in kilograms of carbon dioxide equivalent ($kgCO_2$ eq/t)
- Acidification potential as the impact of the emissions of sulfur and other substances leading to acidification of terrestrial and water bodies in kilograms of sulphur dioxide equivalent (kg SO_2 eq/t)
- Abiotic depletion potential as the depletion of non-renewable, non-biological resources that are not recreated by nature over an extended period of time such as metals, minerals, and fossils fuels in kilograms of antimony equivalent (kgSb eq/t).
- Eutrophication potential as the substances emitted to nature that can lead to an increase in biological productivity in terrestrial and water bodies, causing abnormally dense growth of plant life in kilograms of phosphate equivalent ($kgPO_4$ eq/t)
- Photochemical ozone creation potential as the creation of ozone at ground level due to the reaction between hydrocarbons and NOx from traffic emissions in terms of kilogram of ethylene equivalents (kgC_2H_4 eq).

The reviewed LCAs explored recycling using various cathode chemistries and under pyro and/or hydrometallurgical processes. Hydrometallurgical processes are less energy consuming than pyrometallurgical ones due to the high energy requirements for smelting metals (Gaines, 2018). In order to further lessen the impact of hydrometallurgy, a recycling facility located near a battery manufacturing facility with a net closed loop for the chemicals, in addition to energy recovery from the battery packs should be used.

The LithoRec group, often cited in this work, undertook a life cycle analysis on their recycling mechanism. Their mechanism differs from the one proposed in this document since their batteries are only discharged electrically and are dismantled manually. However, energy recovery and NMC batteries are considered (Buchert & Sutter, 2016). The work by Olofsson and Romare focuses only on Lithium Iron Phosphate (LFP) batteries recycled by hydrometallurgical processes. Their work does not include the discharge with energy recovery step. Gaines et al.'s 2011 study combines several battery chemistries and material recovery techniques. Gaines' 2018 study focuses on hydrometallurgy for Lithium Cobalt Oxide (LCO) batteries only. Neither of her works include energy recovery from the batteries (Gaines, 2018).

In terms of energy demand, the LithoRec group found that their process provides a net profit, that is saves 47 GJ for every tonne of batteries recycled when compared with landfilling or other conventional end-of-life disposal techniques. Olofsson and Romare found that using recycled materials lessens the energy demand of producing a battery by approximately 50%. Within specific materials, Gaines et al. found recycling reduced the energy demand for producing battery materials by ~70% for aluminium and nickel, ~60% for copper and ~25% for steel. Gaines 2018 found that for the production of cathode materials, there is an almost 50% reduction in energy demand.

The remainder of the categories were only explored in depth by the LithoRec group. They found that their process provides a positive environmental impact in all categories, that is, less toxins are emitted when compared with landfilling or other conventional end-of-life disposal techniques:

- Global warming potential: -2747 $kgCO_2$ eq/t
- Acidification potential: -67$kgSO_2$ eq/t
- Abiotic depletion: -0.35kgSb eq/t
- Eutrophication -4.8 $kgPO_4$eq/t
- Photochemical ozone creation potential: -3 kgC_2H_4 eq/t

From the analyses, it can be seen that recycling has a significantly positive impact on the environment. It is imperative that Li-ion batteries from EVs be recycled. By approximately 2026, an estimated 750'000 EV batteries will be at their end of life (Drabik & Rizos, 2018). Assuming each of those batteries weighs 250kg,

187’500 tonnes of batteries will need to be recycled (Elwert, et al., 2015). If they are, 515’062’500 $kgCO_2$ eq will be mitigated, thereby significantly contributing to the IPCC goals.

5 Conclusion

It has been concluded that there are several options for discharging EV batteries dependent on the state and size of the battery. It has been found that Na_2CO_3 is the strongest candidate for salt solution discharge because it is non-corrosive and relatively cost efficient. It was also found that combining the salt solution discharge and metal powder discharge mechanisms is the most effective means for safely discharging cells to ~0.5V. This process is 'safe' that is, reduces the risk to the recycling facility by minimizing the fire or explosion hazard, minimizes or eliminates human interaction with the battery pack and limits voltage rebound to ~0.5V. The short-circuiting portion of the suggested process is 4 hours, making it in line with the electronic load resistive discharge method however, the entire combined process is longer. The process could be sustainable provided that the waste solution is sufficiently treated and that CO_2 is captured for further use. Due to arcing potential, battery packs larger than 500V and/or at greater than 0% SOC are not suggested for the combined salt solution and metal powder discharge method.

For larger battery packs (> 500V) or battery packs and modules above 0% SOC, regenerative electronic load discharge is suggested. This method is most commonly used in industry for several reasons: the process is 'safe' that is, reduces the risk to the facility by minimizing the fire or explosion hazard and limits voltage rebound to ~0.5V, the process takes 4 hours, it is 'sustainable' that is, has no polluting fluid waste streams and is energy efficient and therefore cost efficient. However, connections to the electronic load are made manually, behind the BMS, providing a severe or fatal risk to the user. Therefore, automation of the connection is strongly suggested.

Future recycling processes should make use of inductive, wireless discharge with vehicle to grid energy recovery. This technology should be coupled with a BMS 'override' feature that would restrict the safety mechanisms within the BMS that halt the discharge at 30% SOC. This process would fulfill all the KPIs and overcome the weaknesses of the previous two mechanisms. However, it is unclear how expensive this method would be to implement therefore, if it would be cost efficient.

Due to the high energy and power density within EV batteries, deep discharging is an important safety step in the pre-treatment process. The techniques suggested by this thesis are not only applicable to EV batteries but also to Lithium-ion batteries of varying applications including portables, other e-mobility, industrial electrification, grid stabilization and renewables. Recycling using energy recovering, hydrometallurgical process reduces greenhouse gas emissions and reduces the amount of toxins released into the environment. Therefore, recycling lithium ion batteries is essential to meeting the IPCC goal of reducing global warming to 1.5˚C.

6 Future Work

- Step-wise scale up from cells to modules to battery packs using the salt-solution/metal powder discharge method to confirm the real-life maximum voltage before arcing
- Introduction of standard inductive discharge pads in EV batteries for ease of recycling
- Introduction BMS 'override' feature for ease of recycling
- Testing of other salts not tested in this document to confirm that Na_2CO_3 is the strongest candidate for the salt-solution/metal powder discharge method
- Confirmation that discharging and short circuiting allows appropriate chemical purity and composition for recycling using hydrometallurgical methods
- Confirmation of the number of cells that can be discharged per litre using the salt-solution/metal powder discharge method
- Analysis of the gas and waste stream after discharging using Na_2CO_3 to determine the appropriate waste treatment that would be required

Bibliography

Alibaba. (2019, March). *Alibaba*. Retrieved from Alibaba: alibaba.com

Andersson, I., & Oddeby, J. (2018). *Development of Wireless Charging Component in Vehicle*. Gothenburg: Chalmers University of Technology.

Aqion. (n.d.). *Electrical Conductivity*. Retrieved from Aqion: http://www.aqion.de/site/130

Archier, P. (2019, May). Personal Correspondence.

Author, N. (2010). *Book Title*. Stockholm: Publishername.

Battery University. (n.d.). Retrieved from Battery University: https://batteryuniversity.com/

Boker , U., Henzinger, T., & Radhakrishna, A. (2014). Battery transition systems. Proceedings of the 41st ACM SIGPLAN-SIGACT Symposium on Principes of Programming Languages.

Boyden, A., Soo, V., & Doolan, M. (2016). The Environmental Impacts of Recycling Portable Lithium-Ion Batteries. *Procedia CIRP*, 188-193.

Brandt, K., & Garche, J. (2019). General Battery Safety Considerations. *Electrochemical Power Sources: Fundamentals, Systems, and Applications*, 1-19.

Buchert, M., & Sutter, J. (2016). *Updated LCA recycling method for LithoRec II for lithium-ion batteries (in German)*. Berlin: Oko-Institut e.V.

Chagnes, A. (2015). *Lithium process chemistry: Resources, extraction, batteries, and recycling*. Amsterdam: Elsevier.

Compton, K. (1927). The Electric Arc. *Transactions of the American Institute of Electrical Engineers*, 868-883.

Conference Series LLC Ltd. . (n.d.). *Global Warming and Its Effects*. Retrieved 2019, from Climate Change Conferences: climatechange.earthscienceconferences.com/events-list/global-warming-and-its-effects

Conte, F., Gollob, P., & Lacher, H. (2009). Safety in the battery discharge design: the short circuit. *3*(4).

DiChristopher, T. (2018). *Electric vehicles will grow from 3 million to 125 million by 2030, International Energy Agency Forecasts*. Retrieved 2019, from https://www.cnbc.com/2018/05/30/electric-vehicles-will-grow-from-3-million-to-125-million-by-2030-iea.html

Diekmann, J., Hanisch, C., Loellhoeffel, T., Schalicke, G., & Kwade, A. (2016). (Invited) Ecologically Friendly Recycling of Lithium-Ion Batteries - the LithoRec Process. *ECS Transactions*, 1-9.

Drabik, E., & Rizos, V. (2018). *Prospects for electric vehicle batteries in a circular economy*.

EasyChem. (n.d.). *Factors that affect an electrolysis reaction*. Retrieved from EasyChem: https://easychem.com.au/shipwrecks-and-salvage/3-electrolytic-cells/factors-that-affect-an-electrolysis-reaction/

Ellis, M. (2019). Personal Correspondence.

Elwert, T., Goldmann, D., Romer, F., Buchert, M., Merz, C., Schueler, D., & Sutter, J. (2015). Current Developments and Challenges in the Recycling of Key Components of (Hybrid) Electric Vehicles. *Recycling*, 25-60.

Gaines, L. (2018). Lithium-Ion Battery Recycling Processes: Research Toward a Sustainable Course. *17*(68).

Gaines, L., Sullivan, J., & Burnham, A. (2011). Life-Cycle Analysis for Lithium-Ion Battery Production and Recycling. *90th Annual Meeting of the Transportation Research Board*. Washington D.C.

Gratz, E., Sa, Q., Apelian, D., & Wang, Y. (2014). A closed loop process for recycling spent lithium ion batteries. *262*.

Hansson, J. (2019, May). Personal Correspondence. (N. Nembhard, Interviewer)

Haynes, W. (2010). Electrical Conductivity of Aqueous Solutions. In W. Haynes, *CRC Handbook of Chemistry and Physics, 91st Edition*.

Herrmann, C., Raatz, A., Mennenga, M., Schmitt, J., & Andrew, S. (2012). Assessment of Automation Potentials for the Disassenbly of Automotive Lithium Ion Battery Systems.

IPCC. (2014). *Working Group III Report 'Climate Change 2014: Mitigation of Climate Change'*. Retrieved 2019, from IPCC.

IPCC. (2018). *IPCC*. Retrieved 2019, from Summary for Policymakers: https://www.ipcc.ch/sr15/chapter/summary-for-policy-makers/

ITECH. (n.d.). IT8300 Series Regenerative DC Electronic Load.

Julien, C., Mauger, A., Vijh, A., & Zaghib, K. (2016). *Lithium batteries: Science and technology*. Springer.

Khan, S. (n.d.). *Induced current in a wire*. Retrieved 2019, from Khan Academy: https://www.khanacademy.org/science/physics/magnetic-forces-and-magnetic-fields/magnetic-field-current-carrying-wire/v/magnetism-12-induced-current-in-a-wire

Kondas, J., Jandova, J., & Nemeckova, M. (2006). Processing of spent Li/MnO2 batteries to obtain Li2CO3. *84*.

Kruger, S., Hanisch, C., Kwade, A., Winter, M., & Nowak, S. (2014). Effect of Impurities caused by a recycling process on the electrochemical performance of Li[Ni0.33Co0.33Mn0.33]O2. *726*.

Kwade, A., & Diekmann, J. (2018). *Recycling of Lithium-ion batteries: The LithoRec Way*. Springer.

Larsson, F. (2014). *Assessment of safety characteristics for Li-ion battery cells by abuse testing*. Gothenburg: Chalmers Univeristy of Technology.

Lenntech. (n.d.). *TDS and Electrical Conductivity*. Retrieved from Lenntech: https://www.lenntech.com/calculators/tds/tds-ec_engels.htm

Lenntech. (n.d.). *Water Conductivity*. Retrieved from Lenntech: https://www.lenntech.com/applications/ultrapure/conductivity/water-conductivity.htm

Li, H.-F., Gao, J.-K., & Zhang, S.-L. (2008). Effect of Overdischarge on Swelling and Recharge Performance of Lithium Ion Cells. *26*.

Li, J., Wang, G., & Xu, Z. (2016). Generation and detection of metal ions and volatile organic compounds (VOCs) emissions from the pretreatment process for recycling lithium-ion batteries. *52*.

LME. (2019, April 23). *LME Cobalt*. Retrieved from London Metal Exchange: https://www.lme.com/en-GB/Metals/Minor-metals/Cobalt#tabIndex=2

LTS Research Laboratories Inc. (2015, June 30). *Safety Data Sheet Lithium Hexafluorophosphate*. Retrieved from LTS Research Laboratories Inc: www.ltschem.com/msds/LiPF6

Mannheim Transportation. (2016). *Bombardier's PRIMOVE Technology Enters Service on Scandinavia's First Inductively Charged Bus Line*. Retrieved 2019, from Bombardier: https://www.bombardier.com/en/media/newsList/details.bt-20161207-bombardier-primove-technology-enters-servi

Maxey, C. (2019). Personal Corrspondence.

McLaughlin, W., & Adams, T. (1999). *United States of America Patent No. US005888463A*.

Nan, J., Han, D., & Zuo, X. (2005). Recovery of metal values from spent lithium-ion batteries with chemical deposition and solvent extraction. *152*.

Nan, J., Han, D., yang, M., Cui, M., & Hou, X. (2006). Recovery of metal calues from a mixture of spent lithium-ion batteries and nickel-metal hydride batteries . *84*.

Ojanen, S., Lundstrom, M., Santasalo-Aarnio, A., & Serna-Guerrero, R. (2018). Challenging concept of electrochemical discharge using salt solutions for lithium-ion batteries recycling. *76*.

Olofsson, Y., & Romare, M. (2013). *Life Cycle Assessment of Lithium-ion Batteries for Plug-in Hybrid Buses.* Gothenburg: Chalmers University of Technology.

Patulny, R. (2019, April). Personal Correspondence.

Perea, A., Paolella, A., Dube, J., Champagne, D., Mauger, A., & Zaghib, K. (2018). State of charge influence on thermal reactions and abuse tests in commercial lithium-ion cells. *Journal of Power Sources*, 339, 392-397.

Poulson, T. (2019, April). Personal Correspondence. (N. Nembhard, Interviewer)

Qian, K., Huang, B., Ran, A., He, Y., Li, B., & Kang, F. (2019). State-of-health (SOH) evaluation on lithium-ion battery by simulating the voltage relaxation curves. *Electrochimica Acta.*

Shaw-Stewart, J. (2019, January 23). Personal Correspondence.

Shaw-Stewart, J., Alvarez-Reguera, A., Greszta, A., Marco, J., Masood, M., Sommerville, R., & Kendrick, E. (2019). Aqueous solution discharge of cylindrical lithium-ion cells. *Sustainable Materials and Technologies*.

Shi, Y., Chen, G., & Chen, Z. (2018). Effective regeneration of LiCoO2 from spent lithium-ion batteries: a direct approach towards high performance active particles. (4).

Shipley, J. (1934). The Evolution of Carbon Dioxide in the A.C. Electrolysis of Sodium Carbonate and Bicarbonate solutions, and the discharge potentials of carbonate and bicarbonate ions. *Canadian Journal of Reserach.*

Shu, J., Shui, M., Xu, D., Wang, D., Ren, Y., & Gao, S. (2012). A comparative study of overdischarge behaviors of cathode materials for lithium-ion batteries. *16*.

Skorucak, A. (n.d.). *What is a short circuit?* Retrieved 2019, from Physlink.com: https://www.physlink.com/education/askexperts/ae470.cfm

Smith, N. W., & Swoffer, S. (2015). *World Intellectual Property Organization Patent No. WO 2015/077080 A1.*

Sonoc, A., Jeswiet, J., & Soo, V. (2015). Opportunities to Improve Recycling of Automotive Lithium Ion Batteries. *29*.

Statista. (2018). *Electricity prices for households in Sweden 2010-2018, semi-anunually*. Retrieved from Statista: https://www.statista.com/statistics/418124/electricity-prices-for-households-in-sweden/

Tachikawa, K., Kesler, M., & Atasoy, O. (2018). Feasibility Study of Bi-directional Wireless Charging for Vehicle-to-Grid. *SAE International.*

Tedjar, F., & Foudraz, J. (2007). *United States of America Patent No. US 207/0196725 A1.*

The Pennsylvania State University. (2014). *A Structure of Cylindrical Lithium-ion Batteries*. Retrieved 2019, from http://sites.psu.edu/pxp940/wp-content/uploads/sites/14275/2014/08/Poowanart_Assignment_4_revised.pdf

Turner, E. (2016). *Electronic loads with regenerative output: Cool, quiet, reliable and green*. Retrieved from Interpro Systems: https://www.electronicproducts.com/Power_Products/AC_DC_Power_Supplies/Electronic_loads_with_regenerative_output_Cool_quiet_reliable_and_green.aspx

Vanysek, P. (2010). Electrochemical Series. In W. Haynes, *CRC Handbook of Chemistry and Physics, 91st Edition.*

Wambsganss, P. (2019, April). Personal Correspondence. (N. Nembhard, Interviewer)

Wang, H. (2013). Study on recycling of spent lithium ion batteries containing cobalt pilot scale experiment (in Chinese).

Wang, M.-M., Zhang, C.-C., & Zhang, F.-S. (2017). Recycling of spent lithium-ion battery with polyvinyl chloride by mechanochemical process. *67*.

WiTricity. (n.d.). Retrieved from http://witricity.com/

Wuschke, L., Jackel, H.-G., Leissner, T., & Peuker, U. A. (2019). Crushing of large Li-ion battery cells. *85*.

Xiao, J., Jia, L., & Xu, Z. (2017). Recycling Metals from Lithium Ion Battery by Mechanical Separation and Vacuum Metallurgy. *338*.

Xu, C., Ouyang, M., Lu, L., Liu, X., Wang, S., & Feng, X. (2017). Preliminary Study on the Mechanism of Lithium-Ion Battery Pack under Water Immersion. *ECS Transactions*, 209-216.

Zheng , X., Zhu, Z., Lin, X., Zhang, Y., He, Y., Cao, H., & Sun, Z. (2018). A Mini-Review on Metal Recycling from Spent Lithium Ion Batteries. *4*(3).

Zumdahl , S., & Zumdahl, S. (2000). *Chemistry 5th Edition.* Boston: Houghton Mifflin Company.